

**Synthesis and Characterization of Chitosan/Graphene Oxide nanocomposites  
for the removal of lead from lead-acid battery's water**



**By**

Fatima Noor Qureshi

224-FBAS/MSES/F14

**Department of Environmental Science**

**Faculty of Basic and Applied Sciences**

**INTERNATIONAL ISLAMIC UNIVERSITY ISLAMABAD**

**2016**





MS  
628.1683  
QUS

- 1. Heavy metals - Environmental aspects
- 2. Water - por. of carbon

**Synthesis and Characterization of Chitosan/Graphene Oxide nanocomposites  
for the removal of lead from lead-acid battery's water**



**Researcher:**

Fatima Noor Qureshi

224-FBAS/MSES/F14

**Supervisor:**

Dr. Rukhsanda Aziz

Assistant Professor IIUI

**Co-Supervisor:**

Dr. Tariq Yasir

DCS, PIEAS

**Department of Environmental Science**

**Faculty of Basic and Applied Sciences**

**INTERNATIONAL ISLAMIC UNIVERSITY ISLAMABAD**

**2016**



**Department of Environmental Sciences  
International Islamic University Islamabad**

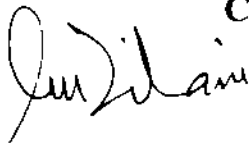
Dated 22 Oct 2017

**FINAL APPROVAL**

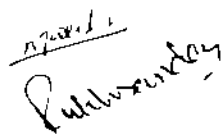
It is certificate that we have read the thesis submitted by Ms (Fatima Noor Qureshi) and it is our judgment that this project is of sufficient standard to warrant its acceptance by the International Islamic University Islamabad for the M S Degree in Bioinformatics

**COMMITTEE**

**External Examiner**



**Internal Examiner**



**Supervisor**

Name

Dr **Rukhsanda Aziz**

Designation

Assistant Professor

Department

Department of Environmental Science

University

International Islamic University

**Co-Supervisor**

Name

Dr Tariq Yasir

Designation

Deputy Chief Scientist

Department

Department of Metallurgy & Materials  
Engineering

University

Pakistan Institute of Engineering & Applied  
Sciences

**Chairperson:**

Name

Dr Rukhsana Tariq

Designation

Assistant Professor

Department

Department of Environmental Science

**Dean, FBAS:**

Prof Dr Muhammad Sher  
Dean FBAS IIUI

A thesis submitted to Department of Environmental Sciences,  
International Islamic University, Islamabad as a partial  
fulfillment of requirement for the award of the  
degree of MS Environmental Sciences

## **Forwarding Sheet**

A thesis entitled "Synthesis and Characterization of Chitosan/Graphene Oxide nanocomposites for the removal of lead from lead-acid battery water" by Fatima Noor Qureshi in partial fulfillment of MS in Environmental Sciences has been completed under my guidance and supervision. I am satisfied with the quality of student's research work and allow her to thesis for further processes per IUU rules and regulations.

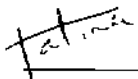
## **DEDICATION**

*This dissertation is dedicated to my beloved parents*

## DECLARATION

I hereby declare that the work present in the following thesis is my own effort, except where otherwise acknowledged and that the thesis is my own composition. No part of the thesis has been previously presented for any other degree.

Date 23-11-2017

  
\_\_\_\_\_  
Fatima Noor Qureshi

# Table of Content

S.No.		Pg. No
	<b>Acknowledgement</b>	<b>i</b>
	<b>List of Abbreviations</b>	<b>ii</b>
	<b>List of Figures</b>	<b>iii</b>
	<b>List of Tables</b>	<b>iv</b>
	<b>Abstract</b>	<b>vii</b>
	<b>Chapter 1</b>	<b>1</b>
1	<b>Introduction</b>	<b>1</b>
1 1	Adsorption	5
1 1 1	Adsorption Models	5
1 1 2	Adsorbent	6
	<b>Chapter 2</b>	
2	<b>Literature Review</b>	<b>8</b>
2 1	Polymer Nanocomposites	9
2 1 1	Chitin & Chitosan	10
2 1 1 1	Properties of Chitosan	11
2 2	Reinforcement	14
2 2 1	Graphene Oxide	14
2 3	Crosslinking	18
	<b>Chapter 3</b>	
3	<b>Materials &amp; Methodology</b>	<b>19</b>
3 1	Chemicals & Solvents	19

3.2	Polymers	19
3.3	Procedure for Synthesis of GO	19
3.4	Procedure for the preparation of Polymer Nanocomposite beads	19
3.5	Procedure for Synthesis of Beads with varying amount of GO	20
3.6	Characterization	21
3.6.1	Infrared Spectroscopy	21
3.6.2	X-Ray Diffraction	22
3.6.3	Surface Area Analysis	22
3.6.4	SEM	22
3.6.5	Thermo gravimetric Analysis	22
3.6.6	Raman Spectroscopy	22
3.7	Batch Adsorption Studies	22
3.7.1	Effect of Time	23
3.7.2	Effect of Adsorbent Dose	23
3.7.3	Effect of pH	23
3.7.4	Effect of Initial Concentration	23
3.8	Statistical Analysis	24
3.9	Adsorption of Electrolyte	24
<b>Chapter 4</b>		
4	<b>Results &amp; Discussions</b>	25
4.1	Synthesis of Graphene Oxide	25
4.2	Characterization of GO	25
4.2.1	Infrared Spectroscopy	25
4.2.2	Raman Spectroscopy	25

4.2.3	Thermogravimetric Analysis	26
4.2.4	SEM	26
4.3	Synthesis of Nanocomposite beads	28
4.4	Characterization of Nanocomposites	29
4.4.1	Infrared Spectroscopy	29
4.4.2	Surface Area Analysis	30
4.5	Adsorption Parameters	31
4.5.1	Effect of Contact Time	31
4.5.2	Effect of pH	32
4.5.3	Effect of Adsorbent Dose	33
4.5.4	Effect of Initial Concentration	33
4.6	Adsorption of Electrolyte	34
5.	<b>Conclusion</b>	35
	References	

## ACKNOWLEDGEMENTS

All the praises and thanks for the creator, **Almighty** countless salutations upon **Prophet Muhammad PBUH**

There are too many debts to repay, firstly I am thankful to **IIUM** that provided me opportunity to achieve **My** objective

I am also grateful to my supervisor **Dr Rukhsanda Aziz** whose understanding guidance made me possible to write down this dissertation

I am hugely indebted to **Dr Tariq Yasin** (co-supervisor **DCS** **PIE**, **PIEC**) whose expertise, guidance, help and skills were there throughout my research work. It was huge pleasure working with you sir

I am highly indebted and thoroughly grateful to **Ms. Saira Bibi** (Ph D scholar) for her immense interest, affection and generous help in my research work. I am also very much grateful to **Mr. Inaam-ul-Hassan** for his sincere advices, guidance throughout my research work, to **Mr Afif Kamal** and **Ms Shaista Taimur** for providing moral supports during my tough times. Words can never be enough to thank your kindness. I don't think I can ever repay the debt I owe you.

I would like to thank **Dr. Mansha Choudhary** (**CS** **PIE**) and **Mr. Islam Khattak** for their generous help. Chairperson, Department of Environmental Sciences, Fatima Jinnah Women University. **Dr Shazia Iftikhar** and **Ms Irum Aziz** for analysis of my samples.

Last but not the least I owe great gratitude for my friend **Quratulain** and **Mehvish Huma** for their love, moral support and help whenever I am in need of and to all classmates/lab mates who supported me all the way.

Fatima Noor Qureshi

## List of Abbreviation

<b>ATSDR</b>	Agency for Toxic Substance and Disease Registry
<b>BET</b>	Brunauer–Emmett–Teller
<b>CNT's</b>	Carbon Nanotubes
<b>CS</b>	Chitosan
<b>FTIR</b>	Fourier Transform Infrared Spectroscopy
<b>FESEM</b>	Field Emission Scanning Electron Microscope
<b>GO</b>	Graphene Oxide
<b>MWCNT's</b>	Multi-walled Carbon Nanotubes
<b>M</b>	Molarity
<b>Pb</b>	Lead
<b>SEM</b>	Scanning Electron Microscope
<b>TEOS</b>	Triethoxyorthosilicate
<b>TGA</b>	Thermogravimetric analysis
<b>TEM</b>	Transmission Electron Microscope
<b>VTESi</b>	Vinyltriethoxysilane
<b>XRD</b>	X-ray Diffraction

↓

## LIST OF FIGURES

S No	Title	Page No
Figure 1	<b>Chemical structure of CHITIN and CHITOSAN</b>	10
Figure 2	<b>Applications of CHITOSAN</b>	11
Figure 3	<b>Structure of Graphene and Graphene Oxide</b>	14
Figure 4	<b>Flow-sheet diagram of Synthesis of chitosan/PVA beads</b>	20
Figure 5	<b>Flow-sheet diagram of Synthesis of chitosan/PVA/GO beads</b>	21
Figure 6	<b>FTIR spectra of GO</b>	27
Figure 7	<b>RAMAN spectra of GO</b>	27
Figure 8	<b>Thermograph of GO</b>	27
Figure 9	<b>Photographic image of GO</b>	27

Figure 10	<b>SEM micrographs of GO</b>	27
Figure 11	<b>Figurative illustration of composition of beads</b>	28
Figure 12	<b>FT-IR spectra of pristine Chitosan</b>	31
Figure 13	<b>Comparison of FT-IR spectra of CS/GO nanocomposite beads</b>	31
Figure 14	<b>Photographic images of CS/GO nanocomposite beads</b>	31
Figure 15	<b>Various Adsorption Parameters for the removal of lead</b>	34

## **LIST OF TABLES**

<b>S. No</b>	<b>Title</b>	<b>Page No.</b>
Table 1	<b>Physical and Chemical Properties of Lead</b>	2
Table 2	<b>Advantages and Disadvantages of Conventional Removal Techniques</b>	4
Table 3	<b>Comparison of concentration of lead before and after adsorption of electrolyte</b>	34

## ABSTRACT

Heavy metal contamination is the matter of concern due to its toxic effects on the human beings as well as on the environment. The power shortage in developing countries resulted in the increased usage and production of lead-acid batteries as a cheap alternative power source. The informal recycling of used lead-acid batteries resulted in the increased lead intoxication. In this work, Graphene Oxide has been synthesized using modified Hummer's Method and characterized with the help of instrumental techniques, FT-IR, Raman, SEM and TGA. Chitosan/GO nanocomposites have been prepared and characterized by FT-IR and BET and adsorption efficiency towards the removal of lead (Pb) have been investigated. Adsorption parameters for the removal of lead including, effect of contact time, adsorbent dose, pH and initial concentration have been studied. The characterization results showed the successful synthesis of GO from Graphite as well as the presence of chemical linkages among the polymers and GO. The batch adsorption results showed that the optimum time for the removal of lead for CS/GO-5 and CS/GO-10 are 120 minutes. The optimum value for pH and adsorbent dose is 5 and 10 mg respectively. The removal efficiency for CS/GO-0, CS/GO-5, CS/GO-10 were 69%, 99% and 97% respectively. The above results showed that CS/GO-5 and CS/GO-10 beads have improved removal percent as compared to CS/GO-0 beads. However the difference in removal percent among CS/GO-5 and CS/GO-10 is not significant. The addition of GO thus improved the adsorption efficiency for lead and therefore could be the potential candidates of adsorbents for the removal of lead from wastewaters.

Chapter 1

# Introduction

**Introduction:**

Water is the most valuable natural resource among all others due to its large usage and importance. Fresh, clean and plentiful amount of water serves as the foundations of a prosperous community. Clean water is necessary for the survival of mankind. About two third of the total surface of earth is covered with water, that includes oceans, glaciers, freshwater lakes, rivers and streams (Metcalf & Inc, 1991). Water is a renewable natural resource but its uncontrolled usage makes it an exhaustible resource. freshwater is of great concern because of its large consumption and other issues related to its degradation. Dirty water has become a world's biggest health risk, and affects all types of life on earth (Lee *et al.*, 2005)

Rapid industrialization and man's quest for comfort has resulted in the advancement of science and technology. This development in industrialization, population expansion and urbanization, lead to severe air, water and soil pollution, affecting the overall environment of the earth in many different ways (Huang *et al.*, 2007). The processing of raw materials generates toxic waste products, harmful effluents and noxious by-products along with the finished goods. The toxic pollutants from these industries ultimately end up in our water supplies (Hanaa *et al.*, 2000). These toxic pollutants from the industries have severely affected the eco-environment and human life. Industrial pollutants includes harmful gases ( $\text{NO}_x$ ,  $\text{SO}_x$ ,  $\text{CO}$ ,  $\text{NH}_3$ ), inorganic pollutants including heavy metals (As, Pb, Hg, Cu, etc), organic pollutants including dyes (Azo-dyes), and various bio-toxics (Azeem, 2009). Among these pollutants heavy metals, organic dyes and bio toxics are mostly discharged untreated into water streams, and is the source of water pollution (Niu & Volesky, 2006, Snoeyink, 1990)

Since many years heavy metals have been used in a number of fields. Heavy metal contamination into the water is the matter of concern because of the extreme toxic effects of these metals on the aquatic life, animals and human beings (Smuda *et al.*, 2007). Metals are of special concern mainly because of their non-biodegradability, persistence and bioaccumulation (Unagolla & Adikary, 2015). The pollution due to heavy metals have created ecological crisis. Heavy metals are ubiquitous, they occur in soils, water, plants. Anthropogenic activities like mining dumping of untreated industrial waste also a source of mobilizing the metals into the environment (Duruibe *et al.*, 2007)

Heavy metals are defined as any metallic element with relatively high density ( $> 4\text{gcm}^{-3}$ ) and toxic or poisonous even at lower concentrations (Hanaa *et al.*, 2000). Heavy metal includes lead,

cadmium, zinc, mercury, arsenic, silver, chromium, copper, iron and platinum group elements. Heavy metals are the natural components of earth crust mainly they are present in the form of ores from which they are usually recovered (Duruibe *et al.*, 2007)

Lead is a chemical element from carbon family, its atomic mass is 82. The physical properties of lead have been listed in table 1. Lead commonly exists in two oxidation states  $Pb^{+2}$  and  $Pb^{+4}$ . The divalent nature is relatively more stable in aquatic environment. Lead is highly toxic and is also a cumulative poison (Járup, 2003)

**Table 1** Physical and Chemical Properties of Lead

Physical Appearance	Bluish-white
Atomic Number	82
Mass Number	207.2 gmol <sup>-1</sup>
Melting Point	327°C
Boiling Point	1155°C
Density	11.34 gcm <sup>-3</sup> at 20°C
Crystalline Structure	Face-centered cubic crystalline structure
Malleability	Relatively soft, capable to be bent or shaped
Conductivity	Poor conductor
Corrosion	Resistant to corrosion
Toxicity	Toxic
Solubility	Pure metal is Soluble in acids
Flammability	Non-flammable
Oxidation States	Pb (0), Pb (II), Pb (IV)

Source: <http://www.ncbi.nlm.nih.gov/books/NBK158769/>

Mankind has been using lead for more than 5000 years in various applications including building materials, pigments for ceramics, water pipes etc. Ancient Romans used lead in the form of lead acetate to sweeten old wines. Presently lead has been extensively used in many different industries such as storage-battery industry (G. Urel *et al.*, 2005)

Lead is very toxic metal and is of great concern mainly because of its persistence. According to ASTDR lead has been recognized as second most hazardous element after Arsenic (ATSDR, 2010). The permissible limit of lead in drinking water according to WHO is  $10\mu\text{gL}^{-1}$ , while according to Pak-EPA  $0.05\text{mgL}^{-1}$  (Snoeyink, 1990). Lead exposure accounts for "almost 1% of the global burden of disease, with the highest burden in developing regions" (Azeem, 2009). Chronic or acute exposure to even small quantities of Lead leads to severe health problems e.g. organ malfunctioning among human beings. It is a broad-spectrum toxin affects all metabolic functions (Hanaa *et al.*, 2000). It has the tendency to accumulate into the tissues, blood and even in the bones and stays for many years. Lead accumulates into the tissues of fishes and other aquatic organisms from water and enters into the food chain (Farooq *et al.*, 2008). Lead can enter into the human bodies through inhalation, drinking water containing lead or eating food contaminated with lead (Mortada *et al.*, 2001, WHO, 1995).

Acute exposure of lead can cause encephalopathy, insomnia, migraine, irritability, convulsion and even coma. The chronic effects of exposure to lead are anemia, kidney disorders, nervous disorders and even death (Steenland, 2000).

The annual worldwide production of lead for the year (2014) was approximately 5.4 million tons and it is also rising with expanding technology (Zahra, 2012). The total amount of lead that has been extracted 60% of it is used by storage battery manufacturing industries specifically automobile battery, remaining of it has been used by paint, pigments industry, ceramic glazing, plastics, ammunition, weights, gasoline additives, solders and many other different products (Zahra, 2012). Once the battery life is ended it became a source of pollution.

Lead acid batteries are the most common and cheap of all the rechargeable batteries and have been extensively used as car batteries and until recently their use as alternate source of electricity in developing countries have also been increased (Bahadır *et al.*, 2007). Lead acid batteries are composed of lead plates as electrodes that are dipped in the bath of sulphuric acid electrolyte, the whole assembly is sealed in polypropylene plastic casing (Bahadır *et al.*, 2007). Lead acid batteries are rechargeable batteries but successive charging and discharging resulted in the lowering the efficiency of batteries due to deterioration of lead plates. Once the units are no longer efficient they are sent to used lead acid batteries (ULAB's) recyclers. During the recycling operations lead has been reclaimed and is sold in a market. In the developing countries like Pakistan the recycling of these batteries is a source of income. But the practices that are

followed for the recycling are informal and generate lead pollution. The plastic seal of batteries are break open with the help of an axe and battery's acid which also contain small amount of lead are simply dumped into the nearby water streams. The lead plates are melted to reclaim useful lead, the melting operation produces lead ash that enters into the air. People living nearby these recycling facilities are greatly exposed to lead contamination (Khan, 2010, Mohammed *et al.* 1996, Roberts 2003). A study from Pakistan has reported that the children of the recyclers and the other people living near these facilities are at a greater risk of overexposure as compared to other people (Khan, 2010).

The increasing demand of pure and fresh water has raised concerns for the conservation and purification of polluted water and to design and environmental friendly, cheap and efficient method for the removal of harmful pollutants.

The conventional methods used for the removal of lead from waste waters can be broadly classified into four classes, chemical precipitation, electrolytic recovery, adsorption, ion exchange, solvent extraction. The methods commonly includes are oxidation reduction, ion exchange, treatment with lime, reverse osmosis, electrolytic recovery (Fan *et al.*, 2013). The advantages and disadvantages of these methods have been listed in the table below.

**Table 2: Advantages and Disadvantages of Conventional Removal Techniques**

Advantages	Disadvantages
<b>Electrodialysis</b>	
<ul style="list-style-type: none"> <li>• Adsorbate ion removal take place with electricity</li> <li>• Less number of chemicals</li> <li>• Generates pure metals</li> </ul>	<ul style="list-style-type: none"> <li>• Removal of chelated ions is not satisfactory</li> <li>• High operational cost</li> <li>• High capital cost</li> </ul>
<b>Chemical precipitation</b>	
<ul style="list-style-type: none"> <li>• Can be used to remove effluent metals</li> <li>• Lesser capital cost</li> </ul>	<ul style="list-style-type: none"> <li>• Cannot be used when metals are present in trace amounts</li> <li>• Generates large amount of toxic sludge is produced</li> <li>• Causes flocculation and sedimentation</li> </ul>

- Complex breaks and adjustment of PH is necessary

### **Ion exchange**

Can facilitate adsorption process.

Regeneration and fouling

High capital and operational cost

### **Adsorption**

- Efficient and economical
  - Remove metals and other pollutants even in trace amounts
  - Simple process, don't generate toxic sludge
  - Lower operational and capital cost
- Needed regeneration

#### **1.1. Adsorption**

Adsorption method is a preferred option among all other because it is relatively simple, cheap, and effective even at lower concentrations of metals and it does not generate any toxic sludge (Musico *et al.*, 2013)

Adsorption is defined as the process of mass transfer in which substance is transferred from the liquid phase to the surface of a solid, and becomes bound either physically or chemically

The substance that is being removed is termed as adsorbate, and the solid, liquid or a gas phase which adsorbs is termed as adsorbent. Adsorption process is broadly classified into two types,

- i Physical adsorption
- ii Chemical adsorption

In physical adsorption, weak forces of attraction like dipole interactions, hydrogen bonding and weak van der waal's forces holds the molecules of adsorbate. Physical adsorption has short equilibrium time and it is also reversible.

In chemical adsorption chemical bonds are responsible for holding the adsorbate molecules. If covalent bond is holding the adsorbate atoms/molecules it termed as weak chemical adsorption, and if it is ionic bond it is called as strong chemical adsorption. It is also irreversible.

The adsorbate molecules are adsorbed in the surface of adsorbent by several mechanisms, ion-pairing (oppositely charged sites), ion-exchange (replacement of counter ions) hydrophobic bonding, polarization of electrons or dispersion forces (Hill, 1959)

### 1.1.1. Adsorption Models:

The measure of adsorbate adsorbed per unit adsorbent mass as a function of the adsorbate equilibrium is expressed by adsorption isotherms. The requisite data for the simulations by different models are derived from adsorption experiments. A known amount of adsorbent is equilibrated with a known concentration and volume of adsorbate. The resulting equilibrium concentration of aliquot is calculated by the following mass balance equation,

$$Q_e = \frac{(C_e - C_o) \times V}{m}$$

Where  $C_o$  is the original concentration of adsorbate,  $C_e$  is the equilibrium concentration,  $m$  is the mass of adsorbent and  $V$  is the volume of the solution

### 1.1.2. Adsorbent:

The choice of suitable adsorbent is very important, a good adsorbent is cheap and easily available, show high selectivity and is reuseable. Surface area, Pore size distribution, surface chemistry and polarity, shape, size are few of the various parameters used to determine the adsorption capability of the adsorbent

Various inorganic materials (charcoal, silica, zeolite, alumina, clay etc) and organic materials (natural and synthetic polymers) as well as the composite of both (polymer nanocomposites) have been used for the adsorption process (Kanchana *et al.*, 2012, Prakash *et al.*, 2012, Zoleikani *et al.*, 2015)

Being hazardous to living organisms, it is essential to remove the toxic heavy metals from potable and waste water by eco-friendly methods, before their utilization and discharge into the environment. Chitosan is a natural polymer, abundantly available and is biodegradable and biocompatible so it is the ideal candidate for the removal of toxic pollutants. The present study will use this low-cost biopolymer chitosan obtained from fisheries waste as an efficient adsorbent for the removal of heavy metal ions

The aim of this study is the synthesis and characterization of novel adsorbent for the removal of Pb(II) from lead storage batteries wastewater

The objectives of the present study are

- To synthesis of Graphene Oxide
- To synthesise and characterize chitosan/graphene oxide nano-composites
- To evaluate the effect of adsorption parameters (pH,dose rate,time of adsorption) on the adsorption of lead from lead-acid battery's water

Chapter 2

# Literature review

Human developments since industrial revolution have resulted in the severe air water and soil pollution. The uncontrolled discharge of pollutants from industries and urban centers has deteriorated the eco-environment (Fan *et al.*, 2013). Among all the harmful contaminants, heavy metals are the most toxic ones. Heavy metals have hazardous effects on both aquatic and terrestrial organisms (Yan *et al.*, 2012, Fan *et al.*, 2013). Lead has been recognized as a longstanding environment contaminant among all the various heavy metals. Various studies have reported the toxic effects of lead.

Falk, 2003 investigated about the Childhood lead poisoning and its health effect. The study revealed that although for years the maximum use of lead has been phased out however many sources that can cause lead poisoning are still there such as, flour mills, lead-glazed ceramics, mining and smelting etc.

Ayana *et al.*, 2008 have also studied the lead exposure among the workers in lead acid battery repair Units of transport service enterprises a case study from Ethiopia. The results of the finding indicated that the average level of Urinary aminolevulinic acid among the workers were significantly high i.e.  $>16\mu\text{g/ml}$ .

Ahmad *et al.*, 2014 searched about the health effects of lead intoxication among the workers of lead-acid batteries industry in Bangladesh. The studies revealed that the informal recycling methods for the recovery of lead is responsible for the unusually high exposure of lead among the workers, the average blood levels were very high. The common illnesses among the workers were headaches, colic pains, nausea, hypertension and anemia. All these diseases were attributable to the high levels of lead exposure.

Among the various methods for the removal of lead adsorption is the most suitable method because of its low-cost and it does not produce toxic sludge or any other type of secondary pollution. The success of metal removal can be achieved only by the choice of suitable adsorbent material, cheap, abundantly available, reusable, non-toxic, biocompatible, biodegradable and having large surface area. Various studies have been carried out for finding suitable adsorbent.

Gercel & Ferdi, 2007 Reported that the Adsorption of lead (II) ions by activated carbon extracted from plant material, *Euphorbia rigida*, adsorption kinetics and various other parameters like pH and temperature have been studied. The calculated maximum adsorption capacity ( $q_{\text{max}}$ ) of lead (II) ions was  $1.35 \times 10^{-3} \text{ mol g}^{-1}$  or  $279.72 \text{ mg g}^{-1}$  at  $40^\circ\text{C}$ .

Xu *et al.*, 2008 Uses Oxidized multiwalled carbon nanotubes (MWCNTs) as sorbent for the removal of Pb(II) from aqueous solution. Adsorption parameters adsorption time, pH, ionic strength, foreign ions, and oxidized MWCNTs' contents under ambient conditions using batch technique have been studied. The results indicate that the efficient removal of Pb (II) from aqueous solution is limited at pH 7–10.

Boudrahem *et al.*, 2011 investigated the efficiency of date tree leaves as a low cost adsorbent for removal of lead ions from aqueous solution. Batch experiments were conducted to study the effects of the main adsorption parameters in detail. The maximum removal of lead(II) is found to be 94 % at pH 5.8, initial Pb(II) concentration of 10 mg L<sup>-1</sup>, adsorbent dose of 1 g L<sup>-1</sup>, agitation speed of 200 rpm, ionic strength of 0.005 M, and temperature of 25 °C.

Azouaou *et al.*, 2013 studied about the efficiency of un-treated orange barks as adsorbent for the removal of Pb<sup>2+</sup>. Batch kinetic and equilibrium experiments were conducted to study the effects adsorption parameters for aqueous solutions of lead. The results revealed that the adsorption was favorable and the maximum adsorption capacity found was equal to 112.36 mg g<sup>-1</sup>.

The use of polymer based nano-composite is an emerging low cost, efficient and cheap adsorbent (Zhu & Schmauder, 2003).

### 2.1 Polymer nano composites:

A composite material is defined as "a combination of two or more chemically distinct phases separated by an interface. The properties of composite material are unique and different from that of its parents. A composite material consists of a matrix phase (greater proportion) and a reinforcing phase/filler that is present in small quantity (Morye *et al.* 1999). There are three types of composites depending upon the type of matrix that has been used.

Metal matrix composite (metal or metal alloy matrix)

- i Ceramic matrix composite (in-organic non metallic material's matrix)
- ii Polymer matrix composite (polymeric matrix)

Polymer nano-composites are composed of a polymeric matrix (natural/ synthetic) and nano-filler are used as a reinforcing agent (Zhu & Schmauder, 2003).

A number of polymeric nanocomposites have been developed and studied for various applications(Cho *et al.*, 2006)

;

Polysaccharides are natural polymers, monomers of polysaccharides are linked together with the help of glycosidase linkage. Polysaccharides easily degrade and their degradation products are non-toxic.

Polysaccharides are classified on the basis of their source as

- i Plant derived polysaccharides
- ii Marine polysaccharides
- iii Extracellular matrix polysaccharides
- iv Polysaccharides derived from microbes

### 2.1.1 Chitin and Chitosan:

Chitin is the second most abundant polysaccharide after cellulose obtained from shells of crustaceans. Chitin is poly- $\beta$ -(1, 4)-linked 2-acetamido-2-deoxy-D-glucopyranose. Chitosan is a derivative of chitin obtained by deacetylation of chitin. When the chitin has degree of deacetylation (DAA) greater than 50% it is termed as chitosan (He *et al.*, 2015). The structure of chitin and chitosan has been shown in figure 1.

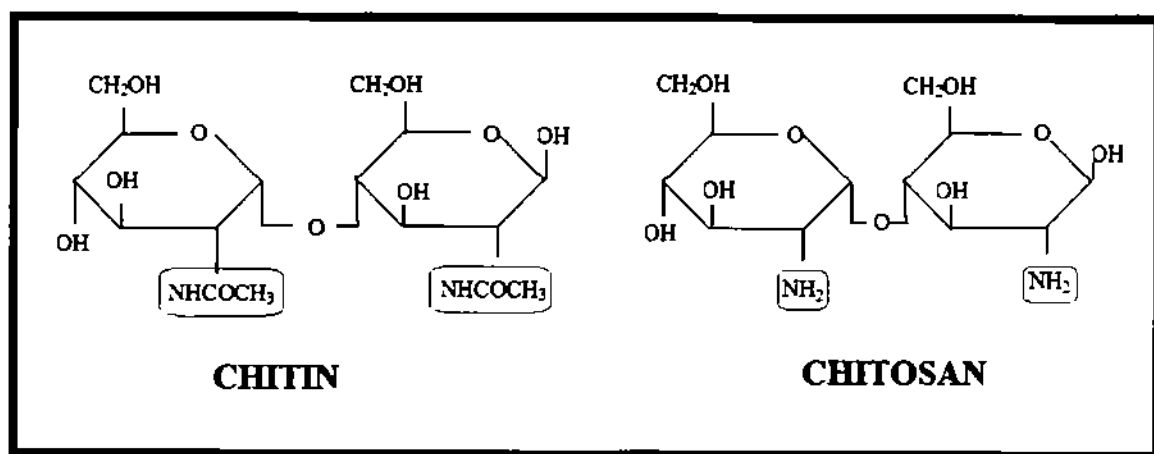


**Figure 1** chemical structure of CHITIN and CHITOSAN

Chitosan was first discovered by Rouget in 1859, the current annual production of chitosan is estimated to be 3000-10,000 tons. It is the only cationic polymer, abundantly available, non-toxic, biodegradable and also biocompatible. It is due to these properties of chitosan that it has been used in polymer nano-composites for various applications (Morley *et al.*, 2006). The various applications of chitosan have been shown in the Figure 2.

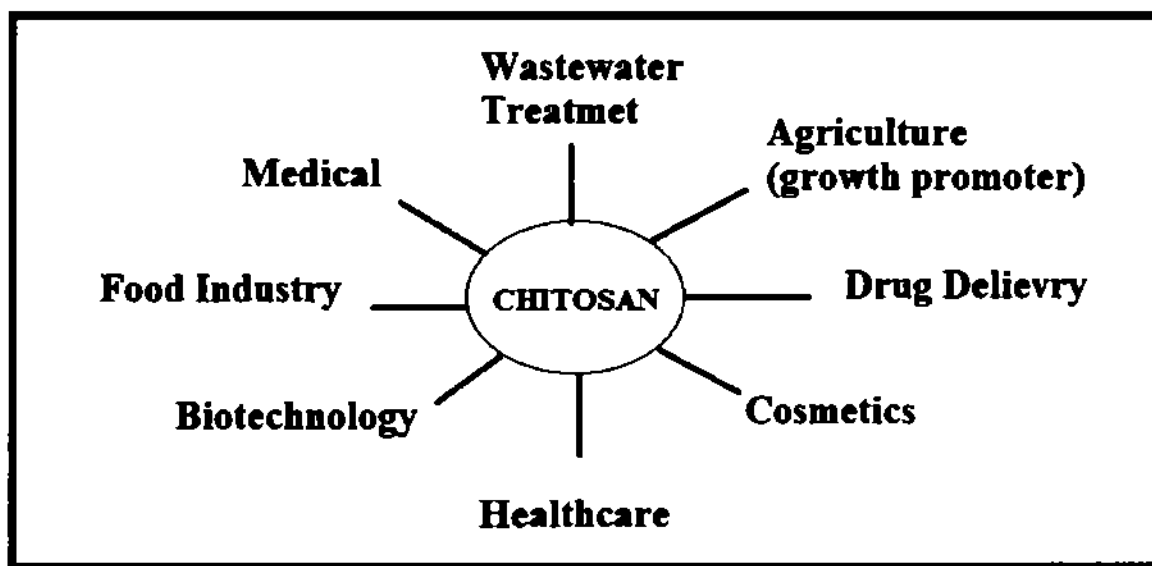


**Figure 2** Applications of CHITOSAN

### 2.1.1.1 Properties of chitosan:

Chitosan is cationic in nature, the amino group protonated in the acidic environment, the protonation occurs at C-2 position of  $\text{NH}_2$  causing solubilisation of chitosan in acids like HCl,  $\text{HNO}_3$  and acetic acid. The pKa value of chitosan is in the range of 6.2-6.8 (Rinaudo, 2006).

Chitosan serves as a metal chelating agent, amino groups on the chitosan chain can react/bind all transition metals from group 3; however, it cannot bind alkali metals as well as alkaline earth metals (Unagolla & Adikary, 2015). In an acidic environment, amino groups are protonated and bind metal ions by ion-exchange (Unagolla & Adikary, 2015).

Chitosan has an ability to adsorb a great variety of metal ions including Cu, Pb, Cd, Hg and a number of dyes as well. Various studies have reported the adsorption efficiency of chitosan derivatives of chitosan and its composites with other biopolymers (cellulose), synthetic polymers (Polyvinyl alcohol), clays (sepiolite, bentonite), carbon nanotubes, graphene/graphene oxide for the removal of heavy metals including lead.

Kamari *et al.*, 2009 studied the adsorption capacities of chitosan and chemically modified chitosan beads for acid dyes. The chitosan was chemically modified with ethylene glycol diglycidyl ether (EGDE) and acid dyes used were Acid Red 37 (AR 37) and Acid Blue 25 (AB 25). Adsorption/Desorption parameters have been studied in detail. Results indicated that the cross-linked chitosan beads showed comparatively lower adsorption than without cross-linked chitosan beads. This is due to the reduction of active sites for adsorption as they were occupied.

by the EGDE molecules. The desorption study data revealed that both cross-linked and uncross-linked chitosan beads retain their adsorption capability after three cycles of adsorption-desorption. Results from FT-IR analysis showed that there is a physical interaction between dyes and chitosan-based adsorbents.

Ngah *et al.*, 2010 synthesized, characterized and studied adsorption abilities of chitosan-tripolyphosphate beads for Pb (II) and Cu (II). The effects of various adsorption parameters have been studied in detail. The maximum adsorption capacities for Pb and Cu were 57.33 and 26.06 mg/g respectively. In binary metal systems the beads were more selective towards Cu over Pb. The thermodynamics parameters showed spontaneous and endothermic in nature. IR spectra were used to explain the mechanism of adsorption.

Prakash *et al.*, 2012 investigated the adsorption abilities of chitosan with Nylon 6 membranes for copper and cadmium ions from synthetic industrial wastewater. Chitosan and Nylon 6 were cross-linked using Glutaraldehyde by blending it with different ratios of glutaraldehyde, 1:1:1:2 and 2:1. The prepared membranes were then used as an adsorbent for the removal of copper and cadmium from wastewater. The prepared were characterized with the help of IR, XRD, TGA/DTA, DSC, and SEM. Adsorption parameters, pH, dose rate, concentration of heavy metal solution and contact time had been done. The results of adsorption parameters showed that the optimal pH is 5 for both the metals and optimum adsorbent dose was 5 g/100 ml for both metals.

Kanchana *et al.*, 2012 synthesized nanocomposites of chitosan, methyl cellulose and clay (kaoline) and enhanced adsorption capacities have been investigated for Pb. Glutaraldehyde was used as a crosslinking agent. The prepared composites were characterized using FTIR, DSC, SEM. FTIR and DSC confirmed the successful synthesis of nanocomposites and SEM micrographs explained the surface morphology of the nanocomposites. The effects of various parameters have been studied in detail. The results showed that nanocomposites of chitosan with kaoline are efficient adsorbent compared to chitosan/ methyl cellulose nanocomposites. The optimum time for adsorption was 300 minutes, optimum adsorbent dose was 6 g L<sup>-1</sup> and optimum pH is 6. The Freundlich isotherm model best explains the adsorption mechanism. The second order kinetic model best explains adsorption kinetics.

Kamal *et al.*, 2014 prepared TEOS cross-linked chitosan/PVA composite beads for the removal of Cu (II) from aqueous solution. The chemical solubility test and the swelling behavior of the beads were studied in acidic media. The prepared beads were instrumentally characterized by

infrared spectroscopy. The results showed that the cross-linking not only improves the mechanical properties and stability of the beads but also preserved active adsorption sites on chitosan. The various adsorption parameters have been studied with the help of batch adsorption experiment. The results indicated the maximum adsorption capacity was 224.6 mg/g according to Langmuir isotherm for  $\text{Cu}^{2+}$  ions. Experimental data best followed Langmuir and Freundlich isotherm models. The thermodynamic parameters suggested endothermic reaction.

Bibi *et al.*, 2015 also prepared chitosan/CNT's nanocomposites and investigated the adsorption properties of the prepared nanocomposites for the removal of poly-aromatic hydrocarbon. The CNT's were  $\gamma$ -treated, irradiated in air at 100kGy. FTIR showed the characteristic peaks of functional groups as well changes in the peaks and intensities. SEM micrograph of chitosan/CNT's nano-composites showed uniform dispersion of CNT's within the polymer matrix. The results of swelling behavior in water and adsorptive removal of naphthalene of the nanocomposites showed that addition of CNT's lowers the swelling ability of the membranes while the membranes uptake 87% of NAPH within first 30 minutes.

Hassan *et al.*, 2016 synthesized, characterized and studied the adsorption behavior of chitosan/Polyvinyl alcohol blends. Methyltrimethoxysilane (MTMS) is used to cross-link the two polymers. Removal of textile dyes (nelson red and palatine orange) has been tested. The prepared membranes were characterized using FTIR. Various adsorption parameters have been studied. The FTIR spectrum confirms the presence of linkages between the two polymers. The maximum dye removal was 1230mg/g and 935mg/g for palatine orange and nelson red respectively. The kinetic data best fits in pseudo first order equation while Langmuir isotherms best explains the mechanism of adsorption. Thermodynamic studies results suggested that the adsorption process was spontaneous and endothermic.

Azaam *et al.*, 2016 prepared chitosan composites with clay, chitosan/clay composites with Ag and Au nano-particles. The prepared nanocomposites were characterized with the help of FTIR, XRD and SEM. Batch adsorption methodology was used to determine the adsorption capacity of prepared nanocomposites for Cu (II). Batch adsorption studies revealed that the adsorption capacity have greatly increased due to addition of Au and Ag nano particles compared to chitosan/clay nanocomposites without nano particles. The maximum adsorption capacity for Cu is 181.5 mg/g.

## 2.2 Reinforcement:

Reinforcements are also called as charge or fillers and in nanocomposites they are in nanoscale are added into the matrix to enhance its mechanical properties and also to lower its cost (Morye *et al.*, 1999) Various forms of reinforcements have been used in polymer matrix e.g. exfoliated clays, glass fibers Carbon nanotubes, carbon nanofibers, Graphene / graphene oxide nano crystalline metals etc

### 2.2.1 Graphene oxide:

Graphene is the new addition to the fascinating carbon family, graphene was first discovered isolated and characterized by Andre Geim and Konstantin Novoselov in 2004, and received "Nobel Prize" in physics in 2010 (Yang *et al.*, 2012)

Graphene is an allotropic form of carbon and is considered as a mother element of some of the allotropes of carbon. It is single sheet of carbon atoms (2-D) arranged in the honey-comb like structure (Tana *et al.*, 2015) (Figure 3)

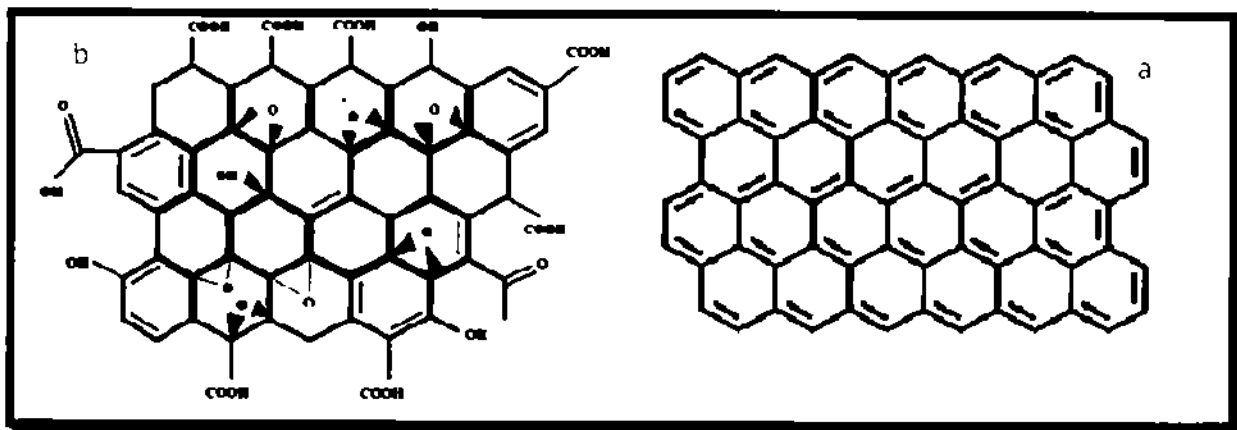


**Figure 3** Structure of Graphene (b) Graphene Oxide (a)

Graphene has excellent mechanical properties, it is the thinnest, strongest and stiffest material in the world as well it is a very good conductor of heat and electricity (Liu *et al.*, 2014) Graphene sheets single atom thick so they have very high surface area and also serves excellent adsorption properties (Hana *et al.*, 2011, Lee *et al.*, 2008)

Graphene oxide is derivative of parent graphene synthesized by the controlled oxidation of graphite Figure 3(b) Graphene oxide is very similar to graphene except it contains oxygen-containing functional groups on its surface (Chen *et al.* 2012) The graphene oxide is prepared by following one of the following developed method Hummer's, Brodie's or Staudmeier. These oxygen-containing functional groups improve their interactions with polar solvents by providing

the polar surfaces as well as reactive groups. Due to high surface area (greater than CNTs) and presence of oxygen containing functional groups make it an excellent adsorbent for the removal of heavy metals and dyes.

Graphene oxide exhibits excellent adsorption abilities but due to dispersion in liquid media its application is limited for the removal of heavy metals. However graphene oxide has very high mechanical strength and has functional groups on the surface so they can be used as reinforcement (nano-fillers) into the polymer matrix (Hana *et al.* 2011).

Fan *et al.*, 2012 synthesized bio-adsorbent made up of magnetic chitosan and graphene oxide (MCGO) for the adsorption of methylene blue. The prepared bio-adsorbent were characterized by Scanning Electron Microscope, IR, X-Ray Diffraction. The effect of various adsorption parameters were also investigated. The results showed higher adsorption capacities and fast kinetics for the removal of Methylene blue. Pseudo second order kinetic model best explains kinetics data and the experimental data followed Langmuir isotherms and Freundlich isotherms.

Yu *et al.*, 2013 synthesized graphene oxide-chitosan aerogels for the removal of Cu ions. The chitosan-graphene oxide composites were lyophilized to prepare aerogels and were adopted as an adsorbent to remove Cu ions. Results indicated the adsorption capacity of aerogels was  $2.54 \times 10$  mg/g calculated by using Langmuir isotherm model. Pseudo second-order model well describes the kinetic data. Intraparticle model predicted the mechanism of adsorption was diffusion. Higher pH values and high temperature favors the adsorption process.

Lia *et al.*, 2014 prepared chitosan/graphene oxide nanocomposites through wet spinning method and their mechanical and dye adsorption properties are being experimented. Batch adsorption experiments were conducted and the effect of adsorption parameters had been investigated. Experimental results indicated that the addition of 4 wt% loading improves the tensile properties of fibers. Adsorption isotherms studies data revealed that Langmuir model best fits to the experimental results and kinetic studies data followed pseudo-second order model. Thermodynamics data suggested that the process of adsorption was spontaneous and exothermic.

Fan *et al.*, 2013 synthesized magnetic chitosan/graphene oxide through a facile and fast process and studied the adsorption application for metal ions. The samples were characterized using FT-IR, TEM, VSM and XRD. The results of characterization confirmed the successful preparation of nanocomposites. The SEM and TEM results showed that magnetic chitosan assembled on the surface of graphene oxide layers. The adsorption ability of magnetic chitosan/graphene oxide

composites had been investigated for lead metals. The maximum adsorption capacity for lead was estimated to be 76.94 mg/g.

Liu *et al.* 2014 reported an easy method for the preparation of PVA/chitosan/Graphene oxide biocomposite nanofibers by electro-spinning. Electron beam irradiation was used to form a homogenous solution of chitosan from chitosan colloidal gel. SEM, Raman spectroscopy was used to characterize the prepared nanofibers. The results of the FESEM showed the uniform distribution on nanosheets of graphene oxide. The average diameter of the biocomposite nanofibers decreases with increase in the percentage of graphene oxide. Mechanical property data revealed that the highest tensile strength was 2.78 MPa and is 25% higher compared with nanofibers without graphene oxide.

Gedam *et al.*, 2015 investigated the adsorption capacity of graphite doped chitosan composites for lead metal. The prepared composites were characterized using following instrumental techniques, X-ray Diffraction, IR and Scanning Electron Microscope. Batch adsorption studies were conducted and various adsorption parameters have been investigated. The results of characterizations confirmed crystalline structure, wide range of porosity, and the presence of C=O and -OH functional groups. Adsorption studies showed that adsorption of lead is highly dependent on pH, maximum uptake of lead was 98% at pH value of 6. 1g/L is the optimum dosage for adsorption and 120 minutes is the optimum time. Langmuir model best explains the mechanism of adsorption and pseudo second order is the best fitted the kinetic data.

Sheshmania *et al.*, 2015 prepared nano-structured composites of chitosan/FeOOH/Graphene oxide. The prepared nanocomposites were characterized by following instrumental techniques, IR, X-ray Diffraction, and Scanning electron microscope and removal of lead by the nanocomposites had been investigated. The results indicated that adsorption process significantly dependent on these parameters.

Ge & Ma, 2015 synthesized chitosan/graphene oxide nanocomposites and its adsorption properties for the removal of chromium ions. The graphene oxide used was modified with triethylenetetramine and the nano-composite was prepared by using microwave irradiation method. The prepared composites were synthesized using following instrumental techniques, FTIR, XRD, SEM, BET and elemental analysis. The results indicated that the prepared composites have high adsorption capacity for chromium as compared with other conventional adsorbents.

available. The maximum adsorption capacity was  $219.5 \text{ mg g}^{-1}$  and the optimum pH value was 2. Adsorption process followed pseudo-second-order kinetic model and Langmuir isotherm models. Moharram *et al.*, 2015 have also prepared and studied adsorption properties of chitosan/graphene oxide nanocomposites. The adsorption properties for lead have been investigated. SEM and FT-IR techniques were used to characterize the prepared composites. Batch adsorption experiments were conducted to study different adsorption parameters. The SEM micrographs indicated that by the addition of graphene oxide to the cross-linked chitosan the surface morphology has changed as it increases the folding and roughness of the composites. The FT-IR spectra further confirmed the chemical interactions between chitosan and graphene oxide. The results of the adsorption studies were as follows: optimum pH was 5, optimum initial dose was found to be 0.2g.

Zhao *et al.*, 2015 synthesized chitosan/graphene oxide hydrogels and investigated the adsorption capacity for dyes. The hydrogels were prepared via self-assembly of chitosan molecules on graphene oxide and were characterized by different instrumental characterization techniques, Raman spectroscopy, SEM, TEM and XRD. The adsorption data indicated the efficient removal of three dye molecules from aqueous solutions, Congo Red dye, Methylene Blue and Rhodamine B. The dye adsorption capacity of the composite hydrogels mainly attributed to the Graphene oxide sheets and chitosan serves for the gelation of graphene oxide sheets.

Wang *et al.*, 2015 investigated the adsorption capacities of magnetic cyclodextrin-graphene oxide nanocomposites for the removal of malachite green from aqueous solutions. The prepared nanocomposites were characterized with the help of FT-IR, TEM, VSM (vibrating sample magnetometer). The effect of adsorption parameters like adsorption time, adsorption temperature, and pH of solution, adsorption kinetics and isotherms were investigated. The results indicated that the maximum adsorption capacity was  $990 \pm 10 \text{ mg/g}$  at  $45^\circ\text{C}$  and the optimum pH was 7. Desorption studies showed adsorption capacity after five adsorption-desorption cycles was greater than 80%. The kinetic data followed pseudo second order kinetics equations and isotherm data followed Langmuir adsorption model.

### 2.3 Cross-linking:

Cross-linking took place when the pendant groups or the backbone of polymer chains forms bonds between different chains of the polymer. It may be a physical interaction or a chemical interaction (ionic/ covalent/ secondary interactions). Different methods and techniques are used

to cross-link polymer chains different cross-linking agents have been used to cross link polymer chains in order to improve its mechanical properties (Xie *et al* 2010)

Chapter 3

# Materials & methods

### 3.1 Chemicals and solvents:

Acetic Acid, Ethanol Triethoxyorthosilicate (TEOS), Vinyltriethoxysilane (VTESi), Sodium Hydroxide (NaOH) Ammonium persulphate, Hydrochloric acid (HCl) and Lead Nitrate  $Pb(NO_3)_2$ , Graphite powder, Sulfuric acid ( $H_2SO_4$ ), Potassium permanganate ( $KMnO_4$ ), Hydrogen peroxide ( $H_2O_2$ ) All chemicals are of analytical grade Distilled water was used in all the preparation

### 3.2 Polymers:

Chitosan (product number 3646, viscosity 200-799 centipoise degree of deacetylation > 75% bulk density 0.15-0.30  $g/cm^3$ ,  $M_w$  115000-135000), for indigenous production of chitosan, crab shells were obtained from Karachi, Pakistan Polyvinylalcohol (98-99% hydrolyzed,  $M_w$  85000-90000)

### 3.3 Procedure for the synthesis of graphene oxide (GO):

Expanded graphite was prepared from commercial graphite by treating it with known volume of concentrated HCl diluted with 25ml of distilled water followed by successive washings to neutralize it Filtered and dried to obtain expanded graphite

Sulphuric acid and phosphoric acid in the ration 9:1 were added into the weighed amount of expanded graphite (1g) in a flask fitted with magnetic stirrer and was stirred on ice bath for 30 minutes at 0°C The temperature was continuously monitored as soon as temperature raised from 0-5°C weighed amount of potassium permanganate was added slowly Remove the ice bath and continued stirring for another half hour, than added 10-15ml of distilled water continue stirring for 15-20minutes Sealed the flask and allowed it to boil for 2 hours at 100°C Then added 15ml of distilled water and 5ml of 30% hydrogen peroxide and allow it to stir for 30 more minutes and decant Then added 20ml of HCl and 60ml of distilled water stirred for 30 minutes Washed neutralized and dried

### 3.4 Procedure for the preparation of polymer nanocomposites beads (CS/GO-0):

The nano-composites were synthesized by using solution mixing method Chitosan was dissolved in 50ml of 2% acetic acid solution in a flask fitted with magnetic stirrer at room temperature PVA (Polyvinylalcohol) was dissolved separately in 40ml of distilled water at 80°C under reflux to get a clear solution The dissolved PVA was then added into the chitosan solution under stirring at room temperature for half hour Then added 2% hydrolyzed vinyltriethoxysilane and weighed amount of initiator dissolved separately in 2ml of distilled

water allowed it to heat for 2 hours at 80°C. After 2 hours of continuous stirring 2% TEOS (triethoxyorthosilicate) was added and allowed to stir for another hour at 45°C and sonicated for 1 hour at room 45°C.

The beads were prepared by dropping prepared blend into precipitation bath (10% solution of sodium hydroxide) with the help of a syringe and then washed with plenty of distilled water to neutralize the beads and store it in air tight glass container.

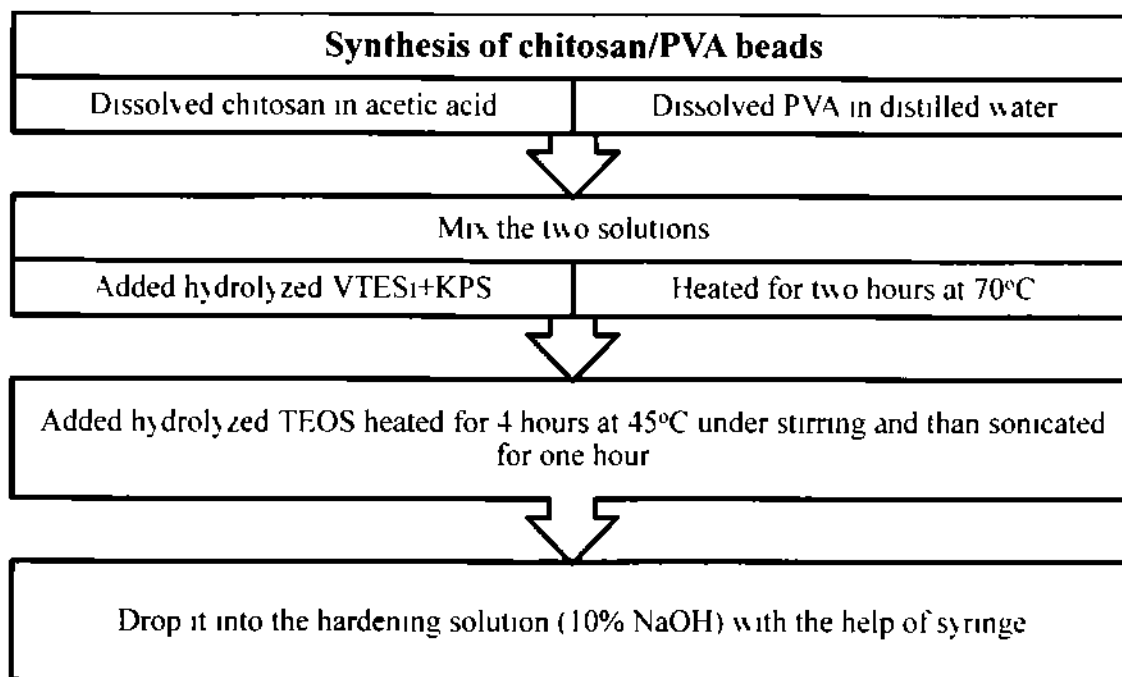


**Figure 4 : Flow-sheet diagram of Synthesis of chitosan/PVA beads**

### 3.5 Procedure for the synthesis of beads with varying amount of graphene oxide (CS/GO-5, CS/GO-10):

The nano-composite were synthesized by using solution mixing method. The weighed amount of Graphene oxide (0.05g, 0.10g, 0.15g) was sonicated in ultrasonic bath for 5 hours to ensure uniform dispersion of Graphene oxide. The sonicated graphene oxide was then added in to the PVA solution and stirred for one hour and then sonicated for one hour at room temperature. Then added chitosan solution into PVA/Graphene oxide blend and again stirred for half hour at room temperature to ensure uniform mixing of the two polymers. Then added 2% hydrolyzed vinyltriethoxysilane (VTESI) and weighed amount (0.02g) of initiator (Ammonium persulphate).

dissolved separately in 2ml of distilled water allowed it to heat for 2 hours at 80°C After 2 hours of continuous stirring 2% hydrolyzed triethoxyorthosilicate (TEOS) was added and allowed to stir for another hour at 45°C and sonicated for 1 hour at 45°C The beads were prepared as mentioned above

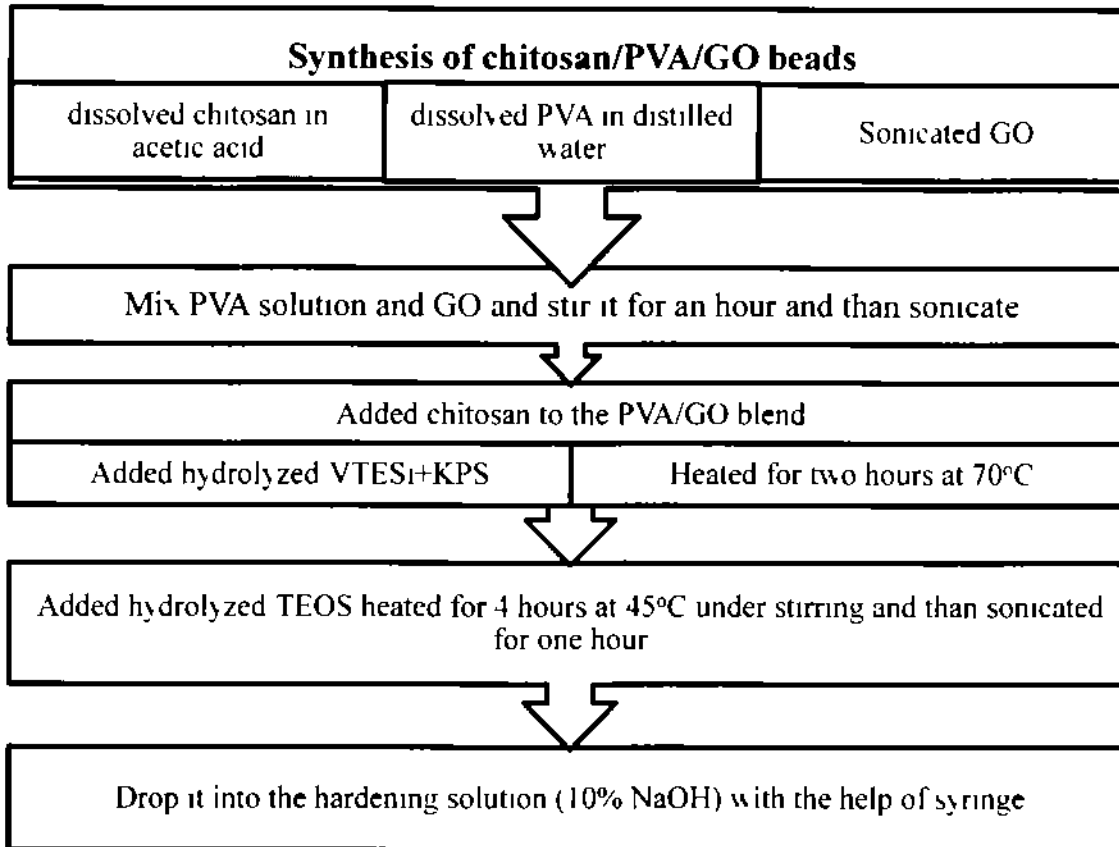


**Figure 5 : Flow-sheet diagram of Synthesis of chitosan/PVA/GO beads**

### 3.6 Characterization:

#### 3.6.1 Infrared spectroscopy

The IR spectra of Graphene and beads were recorded on FT-IR spectrophotometer at room temperature FT-IR spectrophotometer model Nicolet 6700. Thermo Electron Corp. and Waltham, Massachusetts, USA The scanning range was 4000-500  $\text{cm}^{-1}$ , resolution was 6.0  $\text{cm}^{-1}$  and 116 number of scans

#### 3.6.2 X-Ray Diffraction:

The X-ray diffraction analyses were performed on STOE STADI P power diffractometer at a scanning range was  $2^\circ$  to  $50^\circ$

### 3.6.3 Surface Area Analysis:

Brunauer–Emmett–Teller adsorption/desorption experiments were performed by surface area and porosity analyzer model Autosorb-IC, Quantachrome for determining pore volume, pore size and specific surface area of beads. The ~60 mg samples were degassed at  $70^\circ\text{C}$  for 60 min. All samples were characterized under  $\text{N}_2$  environment by using BJH isotherm equation to the  $\text{N}_2$  adsorption isotherm.

### 3.6.4 SEM:

Tescan, MIRA:3 field emission scanning electron microscope coupled with EDX. The samples were dispersed in ethanol before analysis. The images were analyzed at different magnifications.

### 3.6.5 Thermogravimetric analysis:

Thermo-gravimetric analysis (TGA) were performed using TGA/HT DSC HSS2 from  $0^\circ\text{C}$  to  $1500^\circ\text{C}$  under nitrogen atmosphere.

### 3.6.6 Raman spectroscopy:

Raman spectra were taken using Renishaw inVia Raman microscope (Diode pump solid DPSS) at 532 nm green laser. The analysis was carried out at room temperature. The scanning range was from  $300\text{ cm}^{-1}$  to  $4000\text{ cm}^{-1}$  under ambient condition.

### 3.7 Batch adsorption studies:

Stock solution ( $1000\text{ mg L}^{-1}$ ) of lead nitrate was prepared by dissolving calculated amount of lead nitrate in distilled water. Solution with concentration ranging from  $10\text{ mg L}^{-1}$  to  $500\text{ mg L}^{-1}$  was prepared by diluting the stock solution of  $1000\text{ mg L}^{-1}$ . Batch processes at ambient temperature ( $27^\circ\text{C}$ ) were carried out for adsorption experiments. All the experiments were carried-out in triplicates. The concentration of lead was measured with the help of Flame Atomic Absorption Spectrophotometer (FAAS). The wavelength was 283.3 nm with a slit width of 1.0.

The percentage removal “E” was calculated by difference method as follows,

$$\text{Removal \%} = \frac{C_0 - C_e}{C_0} \times 100$$

The adsorption capacity for Pb(II) have been calculated as follows;

$$Q_e = \frac{(C_0 - C_e) \times V}{m}$$

### 3.7.1 Effect of Time:

Kinetic study was done for the optimization of time for the adsorption of lead nitrate. For kinetic study same amount of (10 mg) of water swollen beads were taken in 11 different glass vials. In each of the glass vials 10 ml of  $10 \text{ mgL}^{-1}$  solution of lead nitrate was added. The vials were shaken for stated time interval (10 minutes to 3 hours) at room temperature. The shaking speed was 140 rpm.

### 3.7.2 Effect of Adsorbent Dose:

The effect of adsorbent dose was studied by varying the amount of beads from 2mg to 20 mg at a fixed initial concentration of  $20 \text{ mgL}^{-1}$  for 2 hours. The rest of the parameters were kept constant.

### 3.7.3 Effect of pH:

The effect of pH was measured by varying pH from 4 to 6. Fixed amount of adsorbent and fixed concentration of adsorbate were agitated for optimized time at pH varied 4 to 6. The samples were collected and analyzed for the amount of lead left by difference method.

### 3.7.4 Effect of Initial Concentration:

For isothermal adsorption experiments fixed amount of adsorbent (beads) were added to the 20 ml solution of adsorbate (lead nitrate), the initial concentration of the adsorbate was varied from  $10 \text{ mgL}^{-1}$  to  $100 \text{ mgL}^{-1}$ .

### 3.8. Statistical Analysis:

All the adsorption parameters were carried out in triplicates and an average and standard error of the triplicate has been calculated

### 3.9. Adsorption of Electrolyte:

- The 100ml of electrolyte was obtained from used lead-acid battery and filtered with the help of whatmann filter paper no 1 to remove suspended particles. The concentration of lead and pH of the solution was determined
- The pH of electrolyte was determined with the help of reference electrode potentiometer
- The pH of electrolyte was adjusted to the optimized pH=4 with the help of 75% solution of ammonia
- 20mg of adsorbent (CS/G0-10) was added into the 20ml solution of electrolyte and was agitated for 120 minutes (optimized) at 140 RPM
- The experiment was carried in triplicates
- After 2 hours of agitation the concentration of lead was determined with the help of FAAS (Flame Atomic Adsorption Spectrophotometer)

## Chapter 4

# Results & Discussions

## 4.1. Synthesis of Graphene Oxide:

Graphene oxide has been prepared by multi-step oxidation process of commercial graphite. The graphite was first converted to expanded graphite to facilitate oxidation process. Sulphuric acid was used as an intercalating agent. The expanded graphite was further expanded with the help of 9:1 ratio of sulphuric acid and phosphoric acid. The slurry was then oxidized with the help of  $\text{KMnO}_4$  and temperature is controlled by ice-bath because it is highly exothermic reaction. After oxidation of graphite to graphite oxide the powdered graphite oxide was dispersed in ultrapure water to separate single sheets of graphene oxide were by ultrasonic bath (Fan *et al.*, 2013).

## 4.2. Characterizations of Graphene Oxide:

### 4.2.1 Infrared Spectroscopy:

The FTIR spectra are the infrared absorption/emission spectrum of IR active compound that can be employed for both the quantitative as well as qualitative analysis of unknown mixture. The FTIR analysis of Graphene oxide was performed to determine the newly added functional groups after oxidation of graphite to graphene oxide. Figure 6 showed the FTIR spectra of GO, the spectra showed characteristic peaks for the carboxyl  $\text{C}=\text{O}$  ( $1713\text{ cm}^{-1}$ ), aromatic  $\text{C}=\text{C}$  ( $1614\text{ cm}^{-1}$ ), alkoxy  $\text{C}-\text{O}$  ( $1028\text{ cm}^{-1}$ ), and hydroxyl  $-\text{OH}$  ( $3121\text{ cm}^{-1}$ ) groups.

The presence of above mentioned peaks is consistent with the previously reported literature (Paulchamy *et al.*, 2015 and Song, 2014) confirming the successful oxidation of graphite to Graphene oxide.

### 4.2.2 RAMAN Spectroscopy:

Raman spectroscopy is an active tool for the characterization of carbonaceous materials. The common characteristic peaks, D band ( $1200\text{ cm}^{-1}$  to  $1450\text{ cm}^{-1}$  (disorder induced band) and G-band ( $1500$  to  $1600\text{ cm}^{-1}$  (graphite band) were corresponded to  $\text{sp}^3$  carbon atoms of the defect structure and  $\text{sp}^2$ -hybridized carbon atoms from the aromatic structures respectively (Bibi *et al.*, 2015). The Raman spectra of graphene oxide showed D-band at  $1346\text{ cm}^{-1}$  and G band at  $1603\text{ cm}^{-1}$  as shown in the figure 7. Houbner *et al.*, reported that the presence of D band at  $1350\text{ cm}^{-1}$  and G band at  $1583\text{ cm}^{-1}$  that has been shifted from  $1580\text{ cm}^{-1}$  (G band) and  $1350\text{ cm}^{-1}$  (D

band) of pristine graphite Raman spectra. There was also significant increase in the intensity of D and G bands from D/G ratio of 0.44 in Graphite to 1.58 in GO.

#### 4.2.3 Thermo Gravimetric Analysis (TGA):

TGA analysis was performed to test the thermal stability of Graphene oxide. Result has been shown in Figure 8. The weight loss occurred in three stages. In the first stage, a roughly 5% weight loss occurred at the temperature of 100°C, primarily due to the loss of water molecules in the graphene oxide. During the second stage, the thermal decomposition of instable oxygen-containing functional groups occurred and there was roughly 20% weight loss, occurring at a temperature of 230°C. Finally, 80% weight loss occurred at 850°C, which was mainly due to the combustion of the carbon skeleton. The analysis results clearly indicated the excellent thermal stability of Graphene oxide. Song *et al.*, 2014 reported thermal stability of GO under nitrogen environment and showed the similar three-step weight loss at 100°C (loss of water molecules), 225°C (decomposition of oxygen-containing functional groups) and 620°C (combustion of carbon skeleton).

#### 4.2.4 Scanning Electron Microscope:

Scanning Electron Microscopy is also another powerful tool to determine the structure and morphology of nanomaterials. The SEM micrographs of synthesized graphene oxide have been shown in Figure 10. The SEM micrographs clearly showed very thin sheets of graphene oxide with smooth surfaces. The FTIR data has already confirmed that the carbon layers of the graphite have been successfully oxidized. The inter-planar spacing between the layers of carbon atoms in graphite has increased due to the implantation of oxygen-containing functional groups on both sides of the graphite sheets, which reduces the inter-sheet van der Waals forces. The sonication further separated these already expanded structures, resulting in the synthesis of Graphene oxide (Lia *et al.*, 2014).

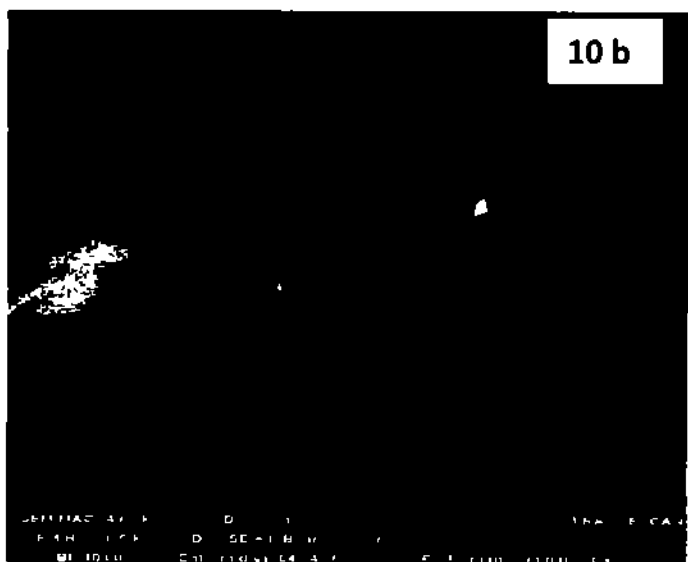
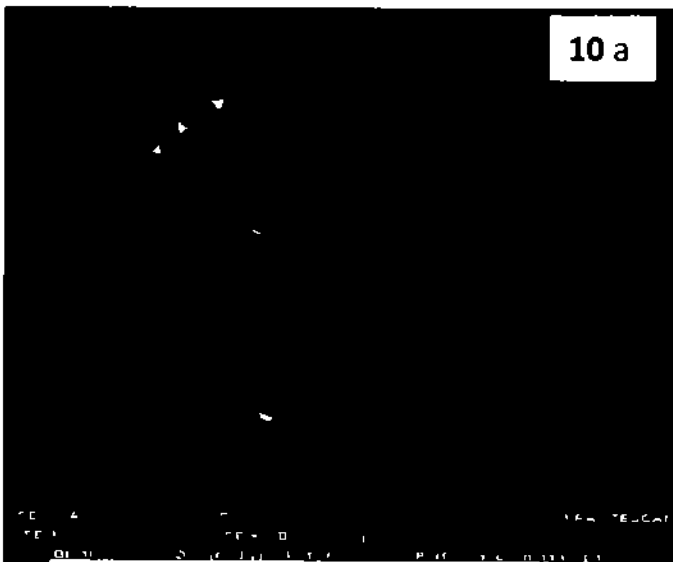
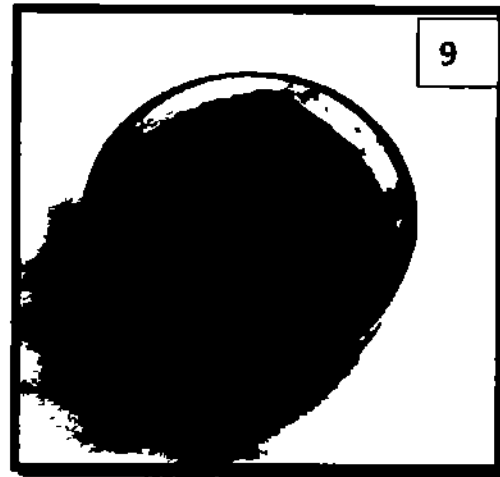
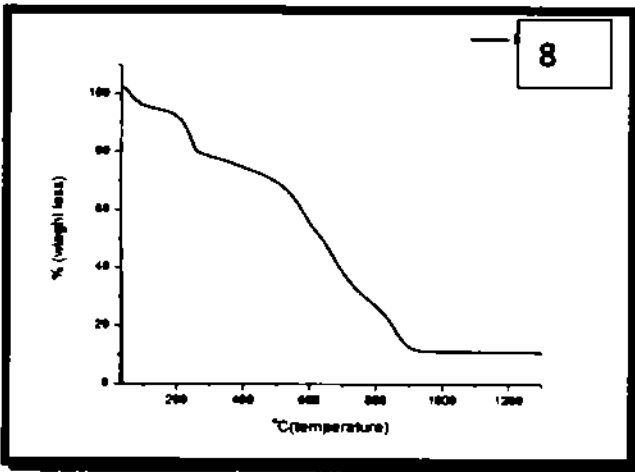
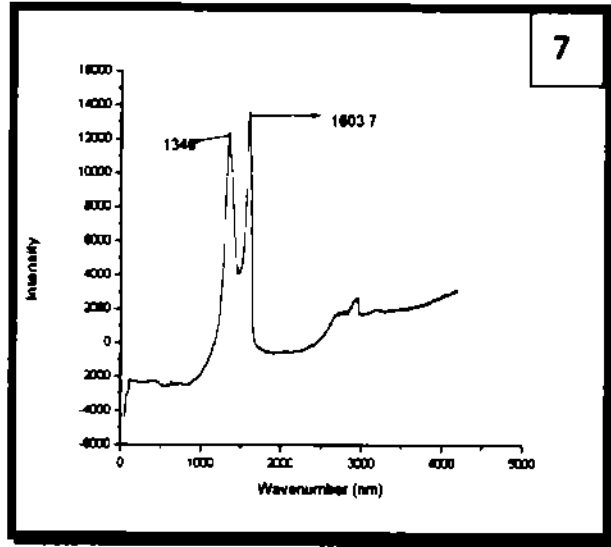
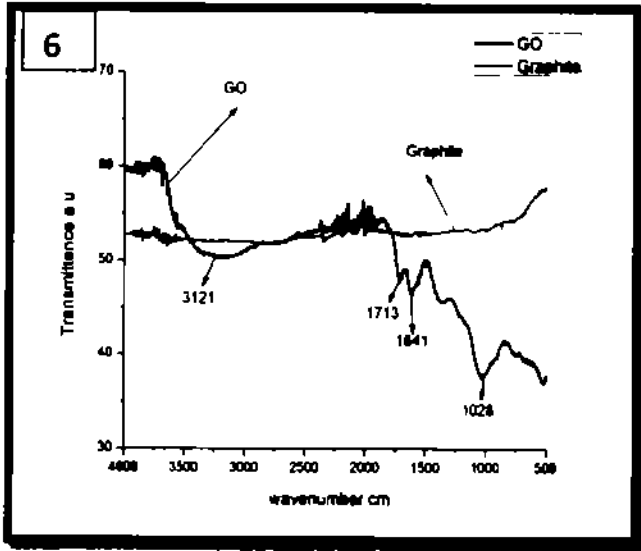


Fig. 6 FTIR of GO Fig. 7 Raman Spectra of GO Fig. 8 TGA of GO Fig. 9 Photographic image of GO  
Fig. 10 a-b SEM images of GO

### 4.3 Synthesis of Nanocomposite beads:

The nanocomposite beads with and without GO were prepared as mentioned in the procedure. The ultrasonic bath was used to ensure the uniform dispersion of GO among the polymer matrix. The results of FTIR discussed below confirmed the presence of chemical interaction between the chitosan and GO. Figure 14 below showed the figurative illustration of composition of CS/GO-5 nanocomposite beads.

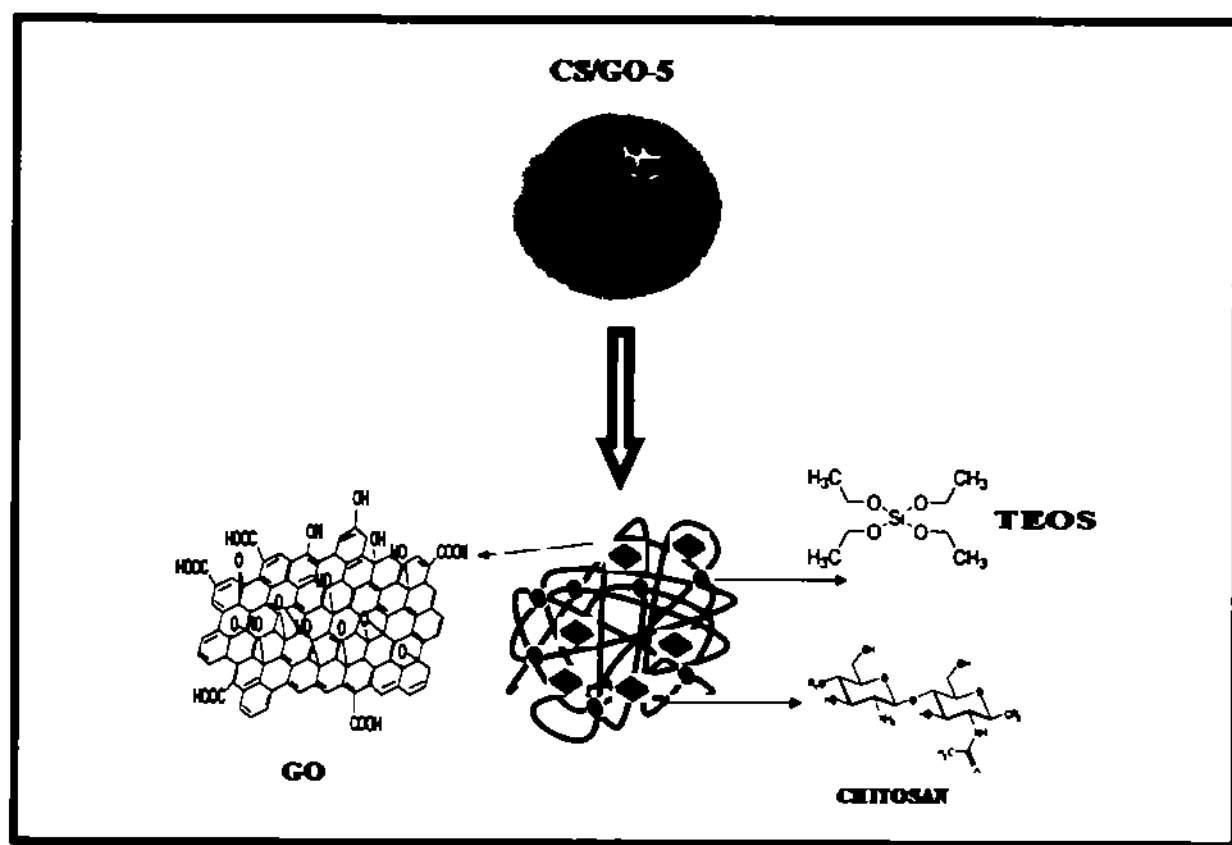


Fig. 11: Figurative illustration of Composition of beads

## 4.4. Characterization of Nanocomposites:

### 4.4.1 Infrared Spectroscopy

The FTIR analysis was performed to investigate the structures, the presence of various functional groups and the type of interactions between different components of the nanocomposites. Fig. 11 showed the FTIR spectra of pristine chitosan. The FTIR spectra of chitosan shows all characteristic peaks that were already reported in the previous literature i.e. A broad peak at  $3290\text{ cm}^{-1}$  of O-H of hydroxyl group N-H symmetric vibration stretching, significant peak at  $2878\text{ cm}^{-1}$  attributed to the C-H stretching vibrations. Two sharp peaks characteristic peak at  $1647\text{ cm}^{-1}$  and  $1585\text{ cm}^{-1}$  carbonyl stretching of amide I (NHCO) and NH bending of amide II group. A sharp peak at  $1378\text{ cm}^{-1}$  and  $1437\text{ cm}^{-1}$  is characteristic peak for  $\text{CH}_2$  bending. Sharp peaks at  $1160\text{ cm}^{-1}$ ,  $1028\text{ cm}^{-1}$  and  $936\text{ cm}^{-1}$  is for anti-symmetric stretching of C-O-C linkage of chitosan monomers and C-O stretching vibration respectively (Burrows *et al.* 2007, Kamal Yasin, Reinert *et al.*, 2016).

FTIR spectra of chitosan/PVA blend after adding graphene oxide have been shown in Fig. 12. The spectrum showed all characteristic peaks with a slight shift. The amide II peak at  $1568\text{ cm}^{-1}$  took blue shift to  $1573\text{ cm}^{-1}$  and  $1578\text{ cm}^{-1}$  after adding 5% and 10% graphene oxide added respectively and the absence of carbonyl stretching peak of COOH in graphene oxide suggested that there may be some interactions between carboxyl group of graphene and  $\text{NH}_2$  group of primary amines, transforming primary amines to secondary amines. The C-N stretching peak shifted to lower intensity due to the reduction in the electron cloud of C-N bond because of the conjugative effect of graphene oxide. The peak shifting and or broadening of the following peaks. The broadening of OH and N-H peaks after the addition of graphene oxide is because of the hydrogen bonding (Kumara & Koha, 2014).

These changes in the characteristic peaks of the composites with and without graphene oxide indicate the interaction between chitosan and graphene oxide.

### 4.4.2. Surface Area Analysis

BET analysis was performed to check the overall surface area of the beads as well as the pore size. The surface area of chitosan/GO beads with 5% and 10% dosage of GO was calculated.

THM 2022

according to BJH isotherm model was 115 516 m<sup>2</sup>/g and 86 822 m<sup>2</sup> g respectively. The pore size and average pore size distribution has estimated by BJH isotherm was 59 5733 nm and 74 5608 nm respectively which indicated that the chitosan/GO beads are macroporous. Fan *et al.*, 2013 have reported the BJH surface area of 382 5m<sup>2</sup>/gat the loading rate of 0.1g of GO. The reduction in the surface area and increase in pore size by the increasing the loading of GO might be due to the agglomeration of Graphene sheets. Kamal *et al.* 2014 have reported BET surface area for CS/PVA beads were very small (0.2-0.5m<sup>2</sup>/g). However the addition of GO to CS/PVA blends have increased the surface area of the beads as shown in the results mentioned above. The increased surface area is responsible for the improved adsorption kinetics.

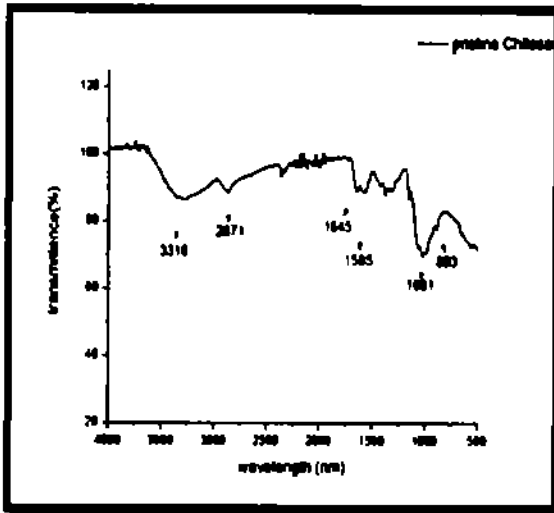


Fig 12 FTIR spectrum of Pristine Chitosan

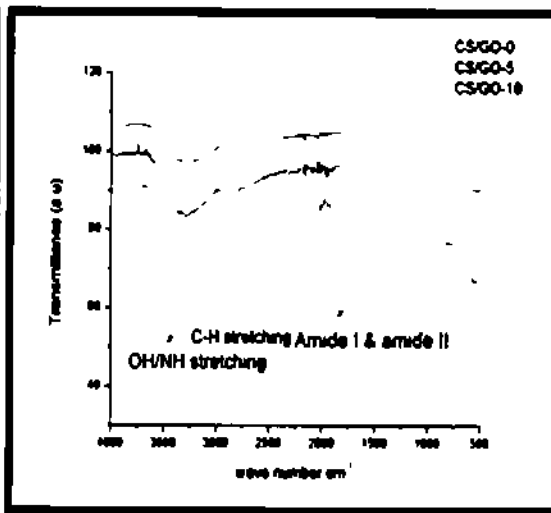


Fig 13 Comparison of FTIR spectra of CS/GO-0, CS/GO-5 CS/GO-10

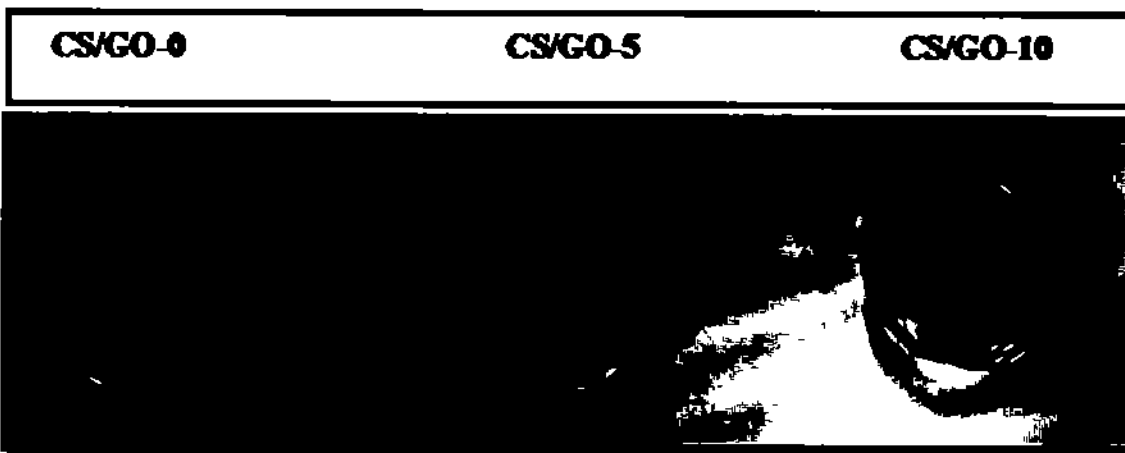


Fig 14 Photographic images of Beads

## 4.5. ADSORPTION PARAMETERS:

### 4.5.1. Effect of Contact Time

Contact Time is one of the very important parameter as it determines the kinetics of the reaction by optimizing time required to reach the equilibrium. A short optimum time means fast kinetics.

and vice versa Fig 15- a showed the effect of time of contact between adsorbent and adsorbate. It is quite clear from the figure that increase in the contact time increases the adsorption capacity /removal percent of lead metal. However the change in adsorption capacity/ removal percent is significant within first 60 minutes of agitation. After 60 minutes the change is not very significant and ultimately equilibrium is achieved after about 120 minutes of agitation. So the optimum contact time for the adsorption of  $Pb^{+2}$  appears to be 120 minutes.

The adsorption of lead occurs following two steps firstly the transfer of metal ions on to the surface of beads and then the attachment of metal ions on to active adsorption sites. During first 60 minutes of contact time a number of adsorption sites are available for binding  $Pb^{+2}$ . After 60 minutes due to gradual decrease of binding sites the rate of adsorption also decreases.

Moharram *et al.*, 2015 have reported that the equilibrium time for adsorption of lead on to CS/GO beads was 300 minutes however the overall trend for adsorption was similar as there was an rapid adsorption initially and decreases gradually until equilibrium is reached.

#### 4.5.2. Effect of pH

The effect of pH is one of the most important parameter as it affects the overall chemistry of the adsorbent as well as adsorbate. Chitosan usually dissolves at lower pH (acidic) value due to the protonation of NH group. The prepared beads were stable at pH value of 4 but pH value less than 4 results in the dissolution of beads and according to the pourbaix diagram for lead,  $Pb^{+2}$  is present in the form of lead hydroxide  $Pb(OH)_2$  at higher pH which readily precipitates so pH  $>4$  &  $<6$  were selected to study the effect of pH on the adsorption of lead (Yu *et al.*, 2013). The effect of pH have been shown in Fig 15-b the removal percentage increases with increase in pH value from 4 to 5 however significantly large removal percent pH 6 might be attributed to the partial adsorption and partial precipitation of lead in the form of lead hydroxide. The trend is similar for all compositions. The relatively low percent removal at lower pH value of 4 may be due to the competition of  $Pb$  ions and  $H^+$  ions have increased and vacancy for the adsorption of  $Pb$  was reduced. However increase in the pH value from 4 to 5 resulted in the increase of percent removal of lead due to the increase in the number of vacancies for  $Pb$ . So the pH value of 5 is selected as the optimum pH for the adsorption of lead. Moharram *et al.*, 2015 have also reported

that the optimum value of pH for the adsorption of lead on Chitosan based adsorbents is 5 (Moharram *et al.*, 2015)

#### 4.5.3. Effect of Adsorbent dose

Effect of adsorbent dose has been investigated by varying the amount of adsorbent keeping rest of the parameters (pH, time and initial concentration) constant. The fig 15- c showed the effect of varying adsorbent dose on the adsorption of  $Pb^{+2}$ . The adsorbent dose was varied from 2mg to 20 mg the figure showed that there is an increase in the percent removal of  $Pb^{+2}$  with increase in the amount of beads from 2mg to 10mg however the increase has become insignificant after increase of adsorbent weight 10mg to 20mg. Similar trend is observed in all of the compositions (CS/GO-0, CS/O-5, CS/GO-10). The increase in the removal percent is attributed to the increase in the number of binding sites by the addition of more adsorbent. At a certain amount since there is no further increase even with increasing amount of adsorbent because of the following two possible reasons (i) Increase in the un-saturation sites (ii) Particle aggregation resulting in the decrease in the total surface area and reduces adsorption capacity. Kamal *et al.*, 2014 and Moharram *et al.*, 2015 have also reported that increase in the weight of adsorbent initially increases the adsorption of Pb. However further increase reduces the adsorption due to the agglomeration of adsorbents (Jin & Bai, 2002, Kamal, Yasin Reinert *et al.*, 2016)

#### 4 5.4. Effect of Initial Concentration

The adsorption efficiency for CS/GO nano-composites have been investigated for Pb by varying the amount of initial concentration of adsorbate. Fig 15-d showed the effect of initial concentration of adsorbate on the removal percent of lead. The concentration of lead was varied from 10 to 100mgL<sup>-1</sup>. As the figure showed with initial rise in the concentration of adsorbate the adsorption capacity also increases however for CS/GO-0 the equilibrium is reached at 50 mgL<sup>-1</sup> of lead nitrate while for CS/GO-5 and CS/GO-10 the adsorption capacity reaches 56mg/g and 64mg/g at 100mg L<sup>-1</sup> of  $Pb^{+2}$  concentration respectively and equilibrium is not reached at 100mgL<sup>-1</sup>. the above mentioned results clearly showed that addition of GO enhances the adsorption capacity of the beads for Pb and increase in the amount of GO from 5% - 10% also improves the adsorption capacity but the increase is not very significant (Fan *et al.*, 2013, Zhao *et al.*, 2015)

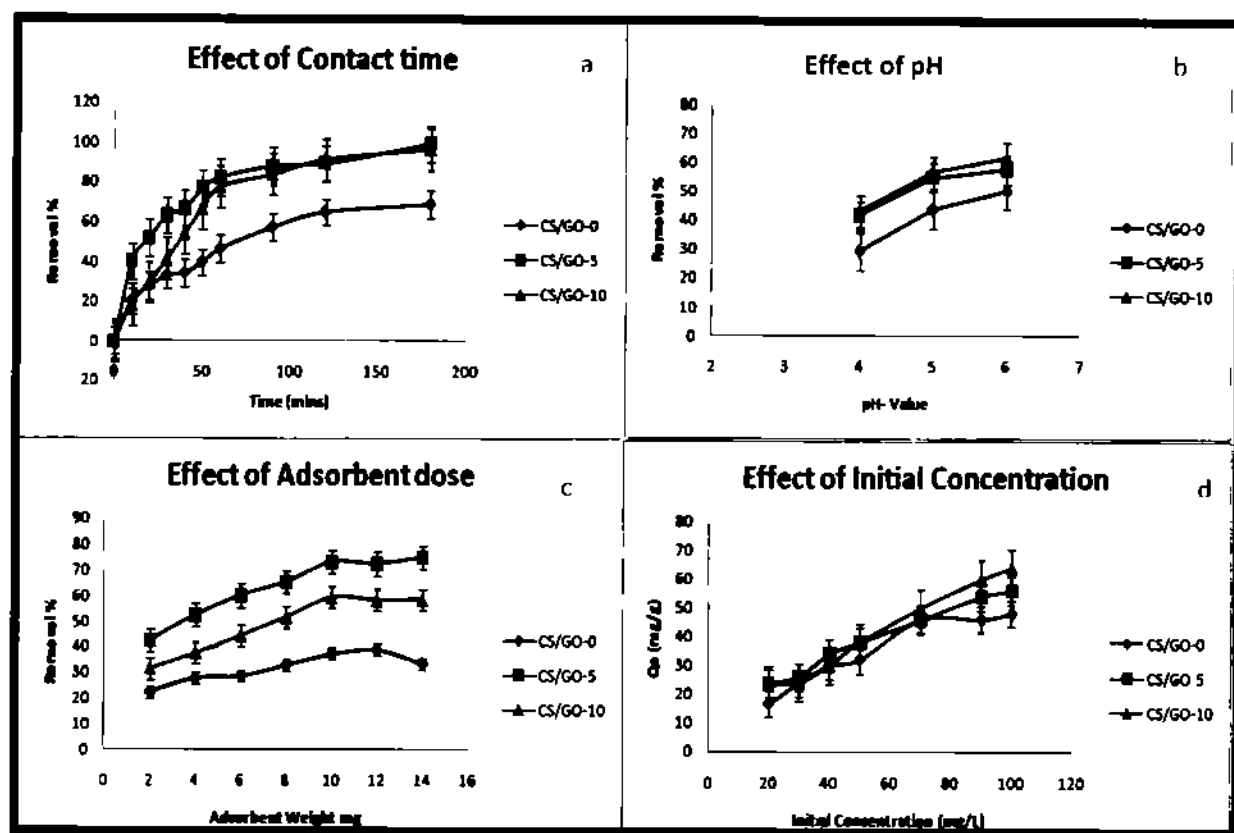


Fig. 15: Various Adsorption Parameters for the removal of lead

#### 4.6. ASORPTION OF ELECTROLYTE:

The electrolyte samples obtained from used lead-acid battery was first analyzed for the amount of lead. The amount of lead present in the electrolyte has been shown in the table 3. The amount of lead in all the three samples were  $< 2 \text{ mgL}^{-1}$  which is also greater than the permissible levels of lead according to Pak-EPA and WHO standards. However after the adsorption of lead through CS/GO-10 nanocomposites using optimized parameters, the level of lead in the electrolyte is almost zero. The above results clearly showed the efficiency of nanocomposites for the removal of lead on the real-time samples. The detailed results have been shown in table 3.

**Table 3: Comparison of concentration of lead before and after adsorption of electrolyte**

S. No	pH of electrolyte		Concentration of lead ( $\text{mgL}^{-1}$ )		Permissible limit of lead (Pb) $\text{mgL}^{-1}$	
	Initial pH	Final pH	Before Adsorption	After Adsorption		
1	<1	3.5	2.34	0.00	Pak-EPA	0.05
2	<1	3.5	2.00	0.00	WHO	0.01
3	<1	3.5	2.28	0.00	US-EPA	0.05

Chapter 5

Conclusions

&

Recommendations

## CONCLUSION

Heavy metal contamination is a worldwide problem and there is need of efficient cost effective and eco-friendly method for the removal of heavy metals. The power shortage in developing countries resulted in the enormous addition of lead acid battery waste resulting in an increased lead contamination.

In the present study a novel, cheap and green adsorbents have been prepared for the removal of lead from wastewater. The adsorbents were prepared from fisheries waste chitosan and was modified with the help of GO. Both products are biocompatible and non-toxic. The characterization of GO and beads confirmed the successful synthesis of GO and CS/GO nanocomposites. The optimum time for adsorption was found to be 120 minutes the optimum pH value was 5. The optimum weight of adsorbent was found to be 10 mg. The removal efficiency was found to be 69%, 99% and 96% for CS/GO-0, CS/GO-5 and CS/GO-10 respectively. The efficiency of nanocomposites was also investigated for real-time samples (electrolyte of used lead-acid battery) and is able to remove lead completely.

The above findings of the research are encouraging and CS/GO can be a potential adsorbent towards the removal of lead.

The loading rate of GO can be further increased to enhance the stability of the beads in acidic media.

The adsorption efficiency of the beads can be checked for other heavy metals like Cu, Cr etc to determine the specificity of the adsorbent towards metals.

The reusability of the adsorbent can be determined by desorption studies.

# References

## REFERENCES

- Ayana, G., Ahmed, K. & Engidawork, E. (2008) Lead Exposure Study among Workers in Lead Acid Battery Repair Units of Transport Service Enterprises, Addis Ababa, Ethiopia: A Cross-Sectional Study *Journal of Occupational Medical Toxicology*(3), 30
- Azeem, H. A. (2009) Analysis of Industrial Waste Water from Kot Lakhpat Area (Lahore, Pakistan) by Atomic Absorption Spectrometer *BIOLOGIA (PAKISTAN)* 55(2), 35-41
- Azouaou, N., Belmedani, M., Mokaddem, H., & Z. Sadaoui. (2013) Adsorption of Lead from Aqueous Solution onto Untreated Orange Barks *The Italian Association of Chemical Engineering*(32), 55-60
- Ahmad, A., Khan, M. H., Khandker, S., Sarwar, A. F. M., Yasmin, N., Faruquee, M. H., & Yasmin, R. (2014) Blood Lead Levels and Health Problems of Lead Acid Battery Workers in Bangladesh [Research Article] *The Scientific World Journal*(2014), 7
- Bahadır, T., Bakan, G., Altas, L., & Buyukgungo, H. (2007) The Investigation of Lead Removal by Biosorption: An Application at Storage Battery Industry Wastewaters *Enzyme and Microbial Technology*( 41), 98-102
- Boudrahem, F., Aissani-Benissad, F., & Soualah, A. (2011) Adsorption of Lead(II) from Aqueous Solution by Using Leaves of Date Trees as an Adsorbent *Journal of Chemical Engineering Data*(56) 1804-1812
- Burrows, F., Loume, C., Abazinge, M., & Onokpise, O. (2007) Extraction and Evaluation of Chitosan from Crab Exoskeleton as a Seed Fungicide and Plant Growth Enhancer *American-Eurasian Journal of Agriculture & Environmental Sciences* 2(2), 103-111
- Bibi, S., Yasin, T., Hassana, S., Riaz, M., & Nawaz, M. (2015) Chitosan/CNT'S Green Nanocomposite Membrane: Synthesis, Swelling and Polyaromatic Hydrocarbons Removal *Materials Science and Engineering C* (46), 359-365
- Chen, Y., Qi, Y., Tai, Z., Yan, X., Zhu, F., & Xue, Q. (2012) Preparation, Mechanical Properties and Biocompatibility of Graphene Oxide/Ultrahigh Molecular Weight Polyethylene Composites *European Polymer Journal*(48), 1026-1033
- Cho, J., Joshi, M. S., & Sun, C. T. (2006) Effect of Inclusion Size on Mechanical Properties of Polymeric Composites with Micro and Nano Particles *Composite Science and Technology*(66), 1941-1952
- Duruibe, J. O., Ogwuegbu, M. O. C., & Ekwurugwu, J. N. (2007) Heavy Metal Pollution and Human Biotoxic Effects *International Journal of Physical Sciences* 2(5), 112-118
- Falk, H. (2003) International Environmental Health for the Pediatrician: Case Study of Lead Poisoning *Pediatrics* 1(112) 259-264

- Fan, L., Luo, C., Sun, M., Li, X., Lu, F. & Qiu, H. (2012) Preparation of Novel Magnetic Chitosan/Graphene Oxide Composite as Effective Adsorbents toward Methylene Blue *Bioresource Technology* (114) 703–706
- Fan, L., Luo, C., Sun, M., Li, X., & Qiu, H. (2013) Highly Selective Adsorption of Lead Ions by Water-Dispersible Magnetic Chitosan/Graphene Oxide Composites *Colloids and Surfaces B Biointerfaces*(103), 523- 529
- Farooq, Y., Hussain, M. M., Aleem, S. B., & Farooq, M. A. (2008) Lead Intoxication: The Extent of Problem and Its Management [Review Article] *Pakistan Journal Physiology*, 4(2)
- Gürel, L., Altas, L., & B. Uyuk, O. H. (2005) Removal of Lead from Wastewater Using Emulsion Liquid Membrane Technique *Environmental Engineering Science*, 22, 411–420
- Ge, H., & Ma, Z. (2015) Microwave Preparation of Triethylenetetramine Modified Graphene Oxide/Chitosan Composite for Adsorption of Cr(VI) *Carbohydrate Polymers*(131), 280-287
- Gedam, A. H., Dongre, R. S., & Banswal, A. K. (2015) Synthesis and Characterization of Graphite Doped Chitosan Composite for Batch Adsorption of Lead (II) Ions from Aqueous Solution *Advance Material Letters* 1(6), 59-67
- Gercel, O. Z. L., & H. Ferdi, G. (2007) Chemical Engineering Journal *Adsorption of lead(II) ions from aqueous solutions by activated carbon prepared from biomass plant material of Euphorbia rigida*(132), 289–297
- Gordon, J. N., Taylor, A., & Bennett, P. N. (2002) Lead Poisoning: Case Studies *British Journal of Clinical Pharmacology*, 5(53) 451–458
- Hana, D., Yana, L., Chen, W., Li, W., & Bangale, P. R. (2011) Cellulose/Graphite Oxide Composite Films with Improved Mechanical Properties over a Wide Range of Temperature *Carbohydrate Polymers*(83), 966–972
- Hanaa, M. S., Eweida, A. E., & Farag, A. (2000) Heavy Metals in Drinking Water and Their Environmental Impact on Human Health *International Center of Economics, Humanities and Management*, 542- 556
- Haubner, K., Morawski, J., Olk, P., Eng, L. M., Ziegler, C., Adolph, B., & Jaehne, E. (in press) The Route to Functional Graphene Oxide [Article]
- He, X., Li, K., Xing, R., Liu, S., Hu, L., & Li, P. (2015) The Production of Fully Deacetylated Chitosan by Compression Method *Egyptian Journal of Aquatic Research*
- Hill, T. L. (1959) Relations between Different Definitions of Physical Adsorption *The Journal of Physical Chemistry*(63) 456–460

- Huang, S. C., Chang, F. C., Lo, S. L., Lee, M. Y., Wang, C. F., & Lin, J. D. (2007) Production of Lightweight Aggregates from Mining Residues Heavy Metal Sludge, and Incinerator Fly Ash *Journal of Hazardous Materials*(144) 52–58
- Hassan, S., Yasin, T., Imran, Z., & Batool, S. S. (2016) Silane Based Novel Crosslinked Chitosan/Poly(Vinyl Alcohol) Membrane Structure Characteristic and Adsorption Behaviour *Journal of Inorganic Organometallic Polymer*(26) 208-218
- Jarup, L. (2003) Hazards of Heavy Metal Contamination *British Medical Bulletin*(68) 167–182
- Jin, L., & Bai, R. (2002) Mechanisms of Lead Adsorption on Chitosan/Pva Hydrogel Beads *Langmuir* 25(18) 9765-9770
- Kamal, M. A., Yasin, T., Reinert, L., & Duclaux, L. (2016) Adsorptive Removal of Copper (II) Ions from Aqueous Solution by Silane Cross-Linked Chitosan/Pva/Teos Beads Kinetics and Isotherms *Desalination and Water Treatment*(57), 4037–4048
- Kamari, A., Saime, W., Ngah, W., & Ken, L. (2009) Chitosan and Chemically Modified Chitosan Beads for Acid Dyes Sorption *Journal of Environmental Sciences*( 21), 296-302
- Kanchana, V., Gomathi, T., Geetha, V., & Sudha, P. N. (2012) Adsorption Analysis of Pb(II) by Nanocomposites of Chitosan with Methyl Cellulose and Clay *Der Pharmacia Lettre* 4( 4 ) 1071-1079
- Khan, D. A. (2010) Lead Exposure and Its Adverse Health Effects among Occupational Workers Children *Toxicology and Industrial Health*
- Kumara, S., & Koha, J. (2014) Physicochemical and Optical Properties of Chitosan Based Grapheneoxide Bionanocomposite *International Journal of Biological Macromolecules*(70), 559–564
- Lee, C. G., Wei, S. D., Kysar, J. W., & Hone, J. (2008) Measurement of the Elastic Properties and Intrinsic Strength of Monolayer Graphene *Science*(321) 385-388
- Lee, M., Cho, K., Shah, A. P., & Biswas, P. (2005) Nanostructured Sorbents for Capture of Cadmium Species in Combustion Environments *Environ. Sci Technol* (39) 8481-8489
- Li, L., Wang, Z., Ma, P., Bai, H., Dong, W., & Chen, M. (2015) Preparation of Polyvinyl Alcohol/Chitosan Hydrogel Compounded with Graphene Oxide to Enhance the Adsorption Properties for Cu(II) in Aqueous Solution *Journal of Polymer Research* (22), 150
- Lia, Y., Suna, J., Dua, Q., Zhangb, L., & Xiaoa, (2014) Mechanical and Dye Adsorption Properties of Graphene Oxide/Chitosancomposite Fibers Prepared by Wet Spinning *Carbohydrate Polymers* (102) 755– 761
- Liu, Y., Park, M., Shin, H. K., Pant, B., Choi, J., Park, Y. W., Kim, H.-Y. (2014) Facile Preparation and Characterization of Poly(Vinyl Alcohol) Chitosan/Graphene Oxide Biocomposite Nanofibers *Journal of Industrial and Engineering Chemistry*(20) 4415–4420

- Metcalf, & Inc. E (1991) *Wastewater Treatment Disposal and Reuse* (3rd ed ) McGraw-Hill, NY
- Mohammed T I, Chang-Yen, I. & Bekele, I (1996) Lead Pollution in East Trinidad Resulting from Lead Recycling and Smelting Activities *Environmental Geochemistry and Health* 3(18), 123–128
- Moharram, M A, Ereiba, K M T, Hotaby, W E, & Bakr A M (2015) Synthesis and Characterization of Graphene Oxide/ Crosslinked Chitosan Nanocomposite for Lead Removal Form Aqueous Solution *Research Journal of Pharmaceutical Biological and Chemical Sciences* 1473
- Morley, K L, Chauve, G, Kazlauskas, R, Dupont, C, Shareck, F & Marchessault R H (2006) Acetyl Xylan Esterase-Catalyzed Deacetylation of Chitin and Chitosan *Carbohydrate Polymers*(63) 310-315
- Mortada, W I, Sobh, M A, El-Defrawy, M M, & Farahat S E (2001) Study of Lead Exposure from Automobile Exhaust as a Risk for Nephrotoxicity among Traffic Policemen *American Journal of Nephrology*(21), 274–279
- Morye, S S, Hine P J, Duckett, R A & Ward I M (1999) A Comparison of the Properties of Hot Compacted Gel-Spun Polyethylene Fibre Composites with Conventional Gel-Spun Polyethylene Fibre Composites *Composite Part A Applied Science and Manufacturing*(30) 649-660
- Musico, Y L F, Santos C M, Dalida, M L P, & Rodrigues D F (2013) Improved Removal of Lead(II) from Water Using a Polymer-Based Graphene Oxide Nanocomposite *Journal of Materials Chemistry* 4(1), 3789
- Niu, H C, & Volesky, B (2006) Biosorption of Chromate and Vanadate Species with Waste Crab Shells *Hydrometallurgy* 84(1) 28-36
- Ngah W S W, & Fatmathan S (2010) Adsorption Characterization of Pb(II) and Cu(II) Ions onto Chitosan-Tripolyphosphate Beads Kinetic Equilibrium and Thermodynamic Studies *Journal of Environmental Management*(91) 958-969
- Paulchamy, B, Arthi, G, & Lignesh, B D (2015) A Simple Approach to Stepwise Synthesis of Graphene Oxide Nanomaterial *Journal of Nanomedicine & Nanotechnology*(1) 6
- Prakash N, Sudha, P N, & Renganathan, N G (2012) Copper and Cadmium Removal from Synthetic Industrial Wastewater Using Chitosan and Nylon 6 *Environmental Science Pollution Research*(19) 2930-2941
- Rinaudo M (2006) Chitin and Chitosan Properties and Applications *Progress in Polymer Science*(31), 603 - 632
- Roberts H (2003) Changing Patterns in Global Lead Supply and Demand *Journal of Power Sources* 1-2(116), 23–31

- Sheshmanian, S Nematzadeha, M A, Shokrollahzadehb S, & Ashorib, A (2015) Preparation of Graphene Oxide/Chitosan/Feooh Nanocomposite for the Removal of Pb(II) from Aqueous Solution *International Journal of Biological Macromolecules*(80) 475-480
- Smuda J Dold, B, Friese, K Morgenstern, P, & Glaesser W (2007) Mineralogical and Geochemical Study of Element Mobility at the Sulfide-Rich Excelstor Waste Rock Dump from the Polymetalliczn-Pb-(Ag-Bi-Cu) Deposit, Cerro De Pasco, Peru *Journal of Geochemical Exploration*(92), 97-110
- Snoeyink, V L (1990) *Water Quality and Treatment* NY American Waterworks Association
- Steenland, K & Boffetta, P (2000) Lead and Cancer in Humans Where Are We Now? *American Journal of Indegmous Medicine*(38), 295-299
- Song, J, Wang, X, & Chang, C -T (2014) Preparation and Characterization of Graphene Oxide *Journal of Nanomaterials*, 6
- Tana, P Sunc, J, Hua, Y, Fanga, Z, Bia, Q, Chena, Y & Chenga, J (2015) Adsorption of Cu<sup>2+</sup> Cd<sup>2+</sup> and Ni<sup>2+</sup> from Aqueous Single Metal Solutions on Graphene Oxide Membranes *Journal of Hazardous Materials*(297), 251-260
- Toxicological Profile for Lead (2010)
- Unagolla J M & Adikary S U (2015) Adsorption Characteristics of Cadmium and Lead Heavy Metals into Locally Synthesized Chitosan Biopolymer *Tropical Agricultural Research* 26(2), 395 - 401
- Wang, D, Liu, L Jiang, X, Yu, J & Chen X (2015) Adsorption and Removal of Malachite Green from Aqueous Solution using Magnetic -Cyclodextrin-Graphene Oxide Nanocomposites as Adsorbents *Colloids and Surfaces A Physicochem Eng Aspects*(466), 166-173
- WHO (1995) Lead Environmental Health Criteria [Report] *World Health Organization Geneva* 165
- Xie, Y Hill C a S, Xiao Z Miltz, H & Mai, C (2010) Silane Coupling Agents Used for Natural Fiber/Polymer Composites A Review *Composites Part A*( 41), 809-819
- Xu, D, Tan, X, Chen, C, & Wang, X (2008) Removal of Pb(II) from Aqueous Solution by Oxidized Multiwalled Carbon Nanotubes *Journal of Hazardous Materials* 1-3(154) 407-416
- Yang S Luo S Liu C & Wei W (2012) Direct Synthesis of Graphene-Chitosan Composite and Its Application as an Enzymeless Methyl Parathion Sensor, *Colloids and Surfaces B Biomterfaces* (96), 75- 79
- Yu, B, Xu, J, Liu, J-H, Yang, S-T, Luo, J, Zhou Q, Liu, Y (2013) Adsorption Behavior of Copper Ions on Graphene Oxide-Chitosan Aerogel *Journal of Environmental Chemical Engineering* 1(4) 1044-1050

- Yu, F., Wu, Y., Ma, J., & Zhang, C. (2013) Adsorption of Lead on Multi-Walled Carbon Nanotubes with Different Outer Diameters and Oxygen Contents: Kinetics, Isotherms and Thermodynamics *Journal of Environmental Sciences*, 25(1), 195-203
- Zahra, N. (2012) Lead Removal From Water by Low Cost Adsorbents: A Review *Pakistan Journal of Analytical and Environmental Chemistry*, 13(1), 01-08
- Zhao, H., Jiao, T., Zhang, L., Zhou, J., Zhang, Q., Peng, Q., & Yan, X. (2015a) Preparation and Adsorption Capacity Evaluation of Graphene Oxide-Chitosan Composite Hydrogels *SCIENCE CHINA Materials*( 58), 811-818
- Zhao, H., Jiao, T., Zhang, L., Zhou, J., Zhang, Q., Peng, Q., & Yan, X. (2015b) Preparation and Adsorption Capacity Evaluation of Graphene Oxide-Chitosan Composite Hydrogels *Science China Materials*(58), 811-818
- Zhu, K., & Schmauder, S. (2003) Prediction of the Failure Properties of Short Fiber Reinforced Composites with Metal and Polymer Matrix *Computational Materials Science*(28) 743-748
- Zoleikani, L., Issazadeh, H., & Zarenezhad, B. (2015) Preparation of New Conductive Polymer Nanocomposites for Cadmium Removal from Industrial Wastewaters *Journal of Chemical Technology and Metallurgy*, 1(50), 71-80